The Plant Cell, Vol. 19: 1649–1664, May 2007, www.plantcell.org

The Senescence-Induced Staygreen Protein Regulates Chlorophyll Degradation [W]

So-Yon Park,[a,1] Jae-Woong Yu,[a,1] Jong-Sung Park,[a,1] Jinjie Li,[a] Soo-Cheul Yoo,[a] Na-Yeoun Lee,[a] Sang-Kyu Lee,[b] Seok-Won Jeong,[c] Hak Soo Seo,[a] Hee-Jong Koh,[a] Jong-Seong Jeon,[b] Youn-Il Park,[c] and Nam-Chon Paek[a,2]

[a] Department of Plant Science and Research Institute for Agriculture and Life Sciences, Seoul National University, Seoul 151-921, Korea

[b] Graduate School of Biotechnology and Plant Metabolism Research Center, Kyung Hee University, Yongin 449-701, Korea

[c] Department of Biology, Chungnam National University, Daejeon 305-764, Korea

Loss of green color in leaves results from chlorophyll (Chl) degradation in chloroplasts, but little is known about how Chl catabolism is regulated throughout leaf development. Using the *staygreen* (*sgr*) mutant in rice (*Oryza sativa*), which maintains greenness during leaf senescence, we identified *Sgr*, a senescence-associated gene encoding a novel chloroplast protein. Transgenic rice overexpressing *Sgr* produces yellowish-brown leaves, and *Arabidopsis thaliana* pheophorbide *a* oxygenase–impaired mutants exhibiting a stay-green phenotype during dark-induced senescence have reduced expression of *Sgr* homologs, indicating that *Sgr* regulates Chl degradation at the transcriptional level. We show that the leaf staygreenness of the *sgr* mutant is associated with a failure in the destabilization of the light-harvesting chlorophyll binding protein (LHCP) complexes of the thylakoid membranes, which is a prerequisite event for the degradation of Chls and LHCPs during senescence. Transient overexpression of *Sgr* in *Nicotiana benthamiana* and an in vivo pull-down assay show that Sgr interacts with LHCPII, indicating that the Sgr-LHCPII complexes are formed in the thylakoid membranes. Thus, we propose that in senescing leaves, Sgr regulates Chl degradation by inducing LHCPII disassembly through direct interaction, leading to the degradation of Chls and Chl-free LHCPII by catabolic enzymes and proteases, respectively.

INTRODUCTION

In autumn, plant leaves generally change in color from green to yellow or red as a result of the breakdown of the green pigment chlorophyll (Chl) combined with carotenoid retention or anthocyanin accumulation. The color change takes place during leaf senescence or accelerated cell death caused by various biotic or abiotic stresses (Matile et al., 1999). Leaf senescence, the final stage of leaf development, is not due to passive destruction but rather is regulated by genetic programs controlling the transition from nutrient assimilation to nutrient remobilization (Hörtensteiner and Feller, 2002; Lim and Nam, 2005). Hence, leaf degreening is regarded as a visible marker for plant programmed cell death processes, although a series of other degenerative metabolisms also occur in senescing leaf cells (Noodén et al., 1997).

Chl catabolism is a multistep pathway. Chls confined to the chloroplast thylakoid membranes are degraded to nonfluorescent Chl catabolites that accumulate in the vacuoles of senescing cells (Matile et al., 1988; Hörtensteiner, 2006). For the complete loss of leaf green color, three consecutive steps acting upstream of porphyrin cleavage are required in the Chl catabolic pathway: first, chlorophyllase converts Chl *a* into chlorophyllide *a* (Chlide *a*); second, magnesium-chelating substance converts Chlide *a* into pheophorbide *a* (Pheide *a*); third, Pheide *a* oxygenase (PaO) converts Pheide *a* into red Chl catabolite. Subcellular fractionation experiments show that chlorophyllase activity is present in the inner envelope membrane of chloroplasts (Brandis et al., 1996; Matile et al., 1997). However, the initial substrate, Chl, is tightly bound to the light-harvesting chlorophyll binding protein I (LHCPI) and II complexes in association with photosystem I and II, respectively, in the thylakoid membranes. This spatial separation between enzyme and substrate has explained the latency of chlorophyllase activity in green leaves and has raised the hypothesis that there is an as yet unidentified Chl carrier in the chloroplast stroma that shuttles between thylakoid and inner envelope membranes for Chl transport (Matile et al., 1997, 1999; Hörtensteiner and Matile, 2004). Satoh et al. (1998) proposed the water-soluble chlorophyll protein (WSCP) as a feasible candidate for a Chl carrier. However, a recent report indicated that WSCP might act as a Chlide transporter during periods of increased Chl synthesis in developing leaves rather than during Chl degradation in senescing leaves (Reinbothe et al., 2004). In higher plants, *Chlorophyllase* (*CLH*) genes encode soluble proteins that are predicted to localize in the cytoplasm, vacuole, or chloroplast stroma (Tsuchiya et al., 1999; Takamiya et al., 2000; Okazawa et al., 2006). In *Arabidopsis thaliana*, At *CLH1* (At1g19670) encodes a putative cytosolic chlorophyllase and is upregulated

[1] These authors contributed equally to this work.

[2] To whom correspondence should be addressed. E-mail ncpaek@snu.ac.kr; fax 82-2-873-2056.

The author responsible for distribution of materials integral to the findings presented in this article in accordance with the policy described in the Instructions for Authors (www.plantcell.org) is: Nam-Chon Paek (ncpaek@snu.ac.kr).

[W] Online version contains Web-only data.

www.plantcell.org/cgi/doi/10.1105/tpc.106.044891

in response to stress and/or senescence-related hormones such as wounding, methyl jasmonate, and coronatine (Benedetti et al., 1998; Tsuchiya et al., 1999; Benedetti and Arruda, 2002). On the other hand, At *CLH2* (At5g43860), which encodes a putative chloroplast chlorophyllase, is constitutively expressed at a low level throughout leaf development, and this expression is unaffected by either stress or senescence (Tsuchiya et al., 1999; Benedetti and Arruda, 2002). However, the gene(s) encoding the inner envelope membrane-bound chlorophyllase has not yet been identified, and it is still unknown which chlorophyllases are involved in the first step of Chl catabolism during leaf senescence.

In this respect, the stay-green (also called nonyellowing) mutants isolated from several plants have been of great interest in elucidating the genetic and biochemical mechanisms of Chl breakdown during leaf senescence. The stay-green trait can be divided into five types on the basis of its behavior during leaf senescence (Thomas and Smart, 1993; Thomas and Howarth, 2000). Compared with the wild type, type A shows delayed induction of senescence, but the rate of Chl degradation is the same as in the wild type after senescence induction. Type B initiates senescence at the same time, but the decrease of Chl content and photosynthetic activity is much slower. Type C retains Chls almost indefinitely in the senescent leaves, although their photosynthetic competence decreases normally during senescence. Type D results in sudden leaf death from drying or freezing. And type E maintains a much higher Chl level throughout leaf development without increasing photosynthetic competence. Thus, the functional stay-green types A and B maintain both leaf greenness and photosynthetic activity much longer, while the nonfunctional stay-green types C, D, and E have persistent leaf greenness without sustaining photosynthetic competence during senescence. In particular, the genetic and physiological characteristics of type C stay-green mutants, which are controlled by either single or double recessive genes, except for the chloroplast gene *cytG* in soybean (*Glycine max*), have been intensively investigated. We previously reported the *staygreen* (*sgr*) mutation in rice (*Oryza sativa*) that is controlled by a single recessive gene (Cha et al., 2002). During vegetative growth, there is no phenotypic difference between the wild type and *sgr*. However, *sgr* maintains leaf greenness much longer during grain filling. Since the photosynthetic competence of *sgr* leaves decreases normally during that period, it is classified as one of the nonfunctional type C stay-green mutants. To date, type C mutants have been reported in several plants: the *senescence-induced deficiency* (*sid*) mutant in *Festuca pratensis* (Thomas and Stoddart, 1975); the *cytG* and d_1d_2 mutants in soybean (Guiamét et al., 1991); the *green flesh* mutant in tomato (*Solanum lycopersicum*) (Cheung et al., 1993; Akhtar et al., 1999); the nonyellowing mutants in *Phaseolus vulgaris* (Fang et al., 1998) and *Dendranthema grandiflora* (Reyes-Arribas et al., 2001); the *oresara10* (*ore10*) mutant in *Arabidopsis thaliana* (Oh et al., 2000); and the *chlorophyll retainer* mutant in pepper (*Capsicum annuum*) (Efrati et al., 2005).

The nonyellowing *sid* mutant of *F. pratensis* accumulates significant amounts of Chlide *a* and Pheide *a* in the senescing leaves and has no PaO activity (Vicentini et al., 1995; Roca et al., 2004), suggesting that Chl dephytylation by chlorophyllases is suppressed by Pheide *a* accumulation in senescing leaves. In *Arabidopsis*, the PaO-impaired mutants, *pao1* and AsACD1, which were induced by T-DNA insertion and antisense silencing of *ACCELERATED CELL DEATH1* (*ACD1*) (Greenberg and Ausubel, 1993), respectively, maintained leaf greenness only during dark-induced senescence (Tanaka et al., 2003; Pružinská et al., 2005). However, the decreased PaO activity in the mutants resulted in age- and light-dependent cell death in mature leaves, possibly due to the accumulation of the photodynamic Chl catabolite Pheide *a* (Pružinská et al., 2003, 2005; Tanaka et al., 2003). Thus, high levels of Pheide *a* in the AsACD1 leaves did not exhibit persistent greenness during natural senescence (Tanaka et al., 2003). Another PaO-impaired mutant in maize (*Zea mays*), *lethal leaf spot-1* (*lls1*), forms several necrotic spots that spread continuously until all of the mature leaves are wilted and bleached (Gray et al., 1997, 2002). The red Chl catabolite reductase–impaired *acd2* mutants in *Arabidopsis* also exhibit spontaneous cell death lesions in mature leaves (Mach et al., 2001). These defective phenotypes demonstrate that genetic lesions associated with the Chl catabolic pathway will ultimately result in cell death in green mature leaves, thus demonstrating that Chl catabolism is tightly regulated throughout plant development. Since the stay-green mutants do not show any age- and/or light-dependent cell death syndrome under natural growth conditions, it has been proposed that, during leaf senescence, the stay-green genes may encode the regulatory proteins triggering Chl catabolism rather than one of the Chl catabolic enzymes (Pružinská et al., 2003, 2005; Tanaka et al., 2003; Hörtensteiner, 2006).

In this article, we report the identification of *Sgr* in rice and characterize its regulatory role in Chl degradation during leaf senescence. We mapped the *sgr* locus to the long arm of chromosome 9 in rice (Cha et al., 2002), identified *Sgr* by a map-based cloning method, and registered the sequence information of *Sgr* and its homologs from other plants with GenBank in 2004. The *sgr* mutation is caused by a single-base change (G295A) in the coding region of *Sgr*, resulting in a missense mutation (V99M). It was recently reported that the stay-green *y* mutant in *Festuca*/*Lolium* forage plants also resulted from a frameshift mutation of a *Sgr* homolog (Armstead et al., 2006). *Sgr* is highly senescence-inducible and encodes a previously uncharacterized chloroplast protein whose amino acid sequence is extremely conserved in higher plants. The overexpression of *Sgr* in transgenic rice and the reduced expression of *Sgr* homologs in the *Arabidopsis pao1* and *acd1-20* mutants demonstrate that Chl degradation is regulated by *Sgr* at the transcriptional level and that *Sgr* transcription is repressed by either an increase of Pheide *a* or a lack of PaO activity in the senescing leaves. We show that the *sgr* mutant exhibits high stability of LHCPI and LHCPII in senescing leaf cells, while other components decay normally. An in vitro pull-down assay shows that Sgr has specific affinity to LHCPI and LHCPII. Through a transient overexpression assay in *Nicotiana benthamiana* and an in vivo pull-down assay, we confirm that Sgr interacts with LHCPII in vivo. Together, our results demonstrate that the Sgr-LHCPII complexes are formed in the chloroplast thylakoid membranes, which may cause LHCPII disassembly for the breakdown of Chls and Chl-free LHCPII subunits by catabolic enzymes and proteases, respectively, in senescing leaf cells.

RESULTS

Characterization of the Rice *sgr* Mutant during Natural and Dark-Induced Senescence

Leaf stay-greenness, a senescence defect in *sgr*, can be detected not only during grain filling but also during vegetative growth when rice plants are incubated in complete darkness (Figures 1A and 1B). During dark-induced, detached leaf senescence, the wild-type *japonica* rice Hwacheong-*wx* turns yellowish-brown, whereas *sgr* maintains leaf greenness much longer due to the slower degradation of Chls (Figures 1C and 1D). This suggests that Chl catabolism in *sgr* is severely retarded but not completely blocked. To dissect the genetic defect of *sgr* in the Chl catabolic pathway, we used reverse-phase HPLC to examine the presence of green Chl catabolites, Chlide *a* and Pheide *a*, in the senescing leaves of *sgr* in darkness (Figure 2). HPLC results showed that Chlide *a* and Pheide *a* are maintained at low levels in both the wild type and *sgr*. However, the levels increase in *sgr* at 4 d after darkness (DAD) and decrease thereafter.

High Stability of LHCP and Thylakoid Membranes in Senescing Leaf Cells of *sgr*

The nonfunctional type C stay-green mutants share a number of unusual features, such as the high stability of Chl binding

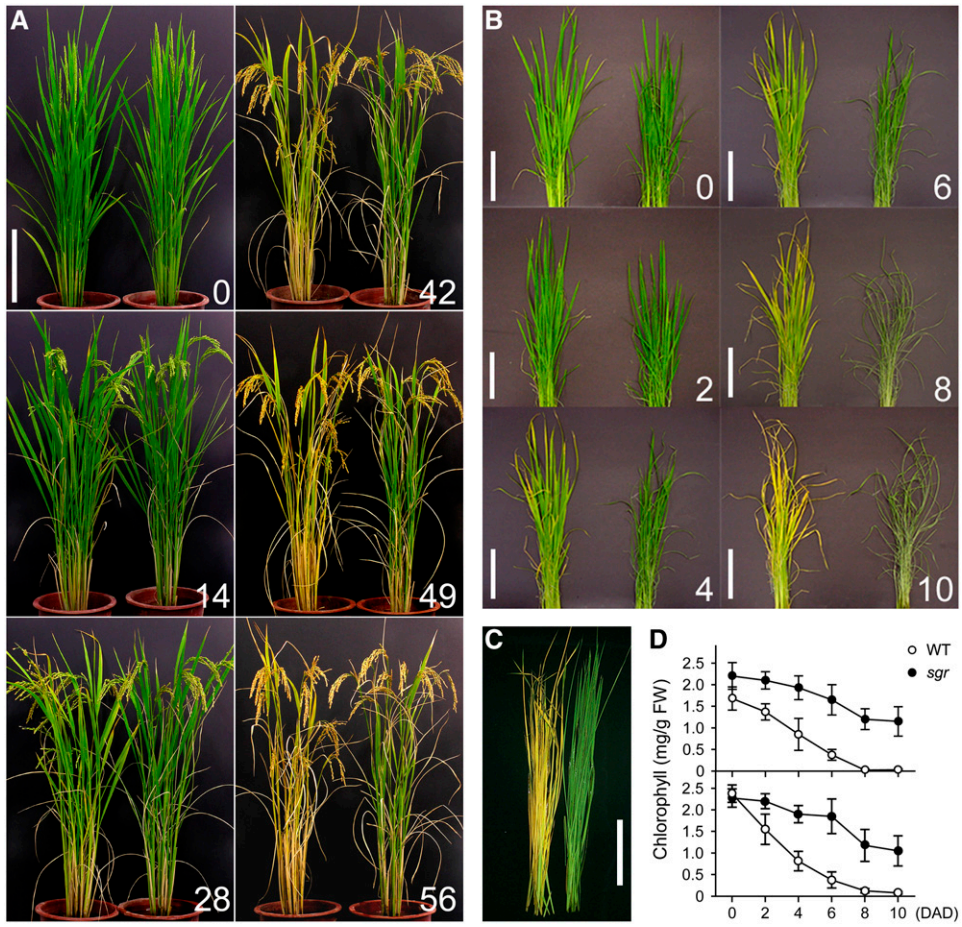

Figure 1. Phenotypic Characterization of *sgr* during Natural and Dark-Induced Senescence.

(A) Changes in leaf color of the wild type (left) and *sgr* (right) during the grain-filling period. Numbers indicate days after heading. The wild type was parental *japonica* cv Hwacheong-*wx*. Bar = 20 cm.

(B) Color changes in attached leaves of the wild type (left) and *sgr* (right) during dark-induced senescence. Two-month-old rice plants grown in a paddy field were transferred to complete darkness at 25°C for 10 d. This experiment was performed more than three times with the same results. Numbers indicate DAD. Bars = 10 cm.

(C) Leaf color phenotypes of excised plants of the wild type (left) and *sgr* (right) after dark incubation. One-month-old plants were excised, placed in moistened plastic bags, and incubated in complete darkness at 30°C for 8 d. This experiment was repeated more than three times with the same results. Bar = 10 cm.

(D) Changes of Chl concentrations in leaves of the wild type and *sgr* during dark incubation. One-month-old (top panel) and 2-month-old (bottom panel) plants were excised and treated as described for **(C)**. Chls were extracted from the leaf tissues. Mean and SD values were obtained from three replications. FW, fresh weight.

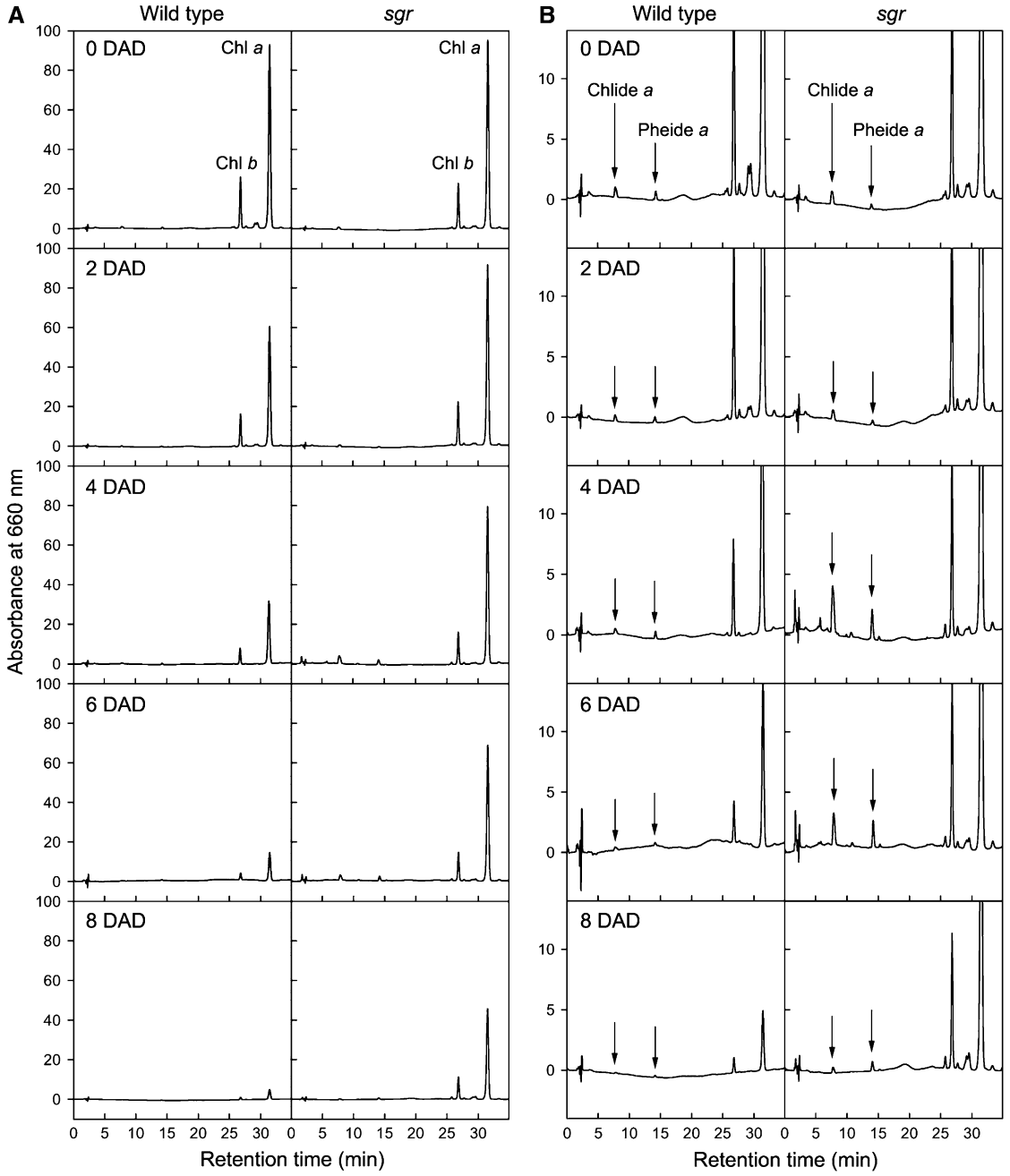

Figure 2. HPLC Results of Chls and Chl Catabolites in Senescing Leaves of the Wild Type and *sgr*.

(A) HPLC results. Two-month-old plants were excised and incubated in complete darkness at 30°C for 8 d, and then Chl derivatives were extracted from leaf tissues for reverse-phase HPLC analysis. Chl *a*, Chl *b*, Chlide *a*, and Pheide *a* were determined at 660 nm with a photodiode array detector. The HPLC analysis was repeated three times with similar results. The wild type was parental *japonica* cv Hwacheong-*wx*.
(B) Enlarged HPLC results from **(A)**.

thylakoid proteins among chloroplast proteins, especially LHCPII, and the persistence of unstacked thylakoid membranes in senescing leaf cells (Thomas, 1977, 1982; Hilditch, 1986; Hilditch et al., 1989; Guiamét et al., 1991; Thomas et al., 2002; Oh et al., 2003). Thus, we further examined the stabilities of thylakoid proteins and membranes in the senescing mesophyll cells of *sgr*. Immunoblot analysis revealed that LHCPI and LHCPII subunits were retained in the senescent leaves of *sgr*, while other thylakoid-bound photosynthetic proteins, D1 and cytochrome *f*, were degraded progressively, as in the wild-type leaves (Figure 3A). Ultrastructural analysis showed that chloroplast degeneration also occurred in *sgr* during senescence but differed to some

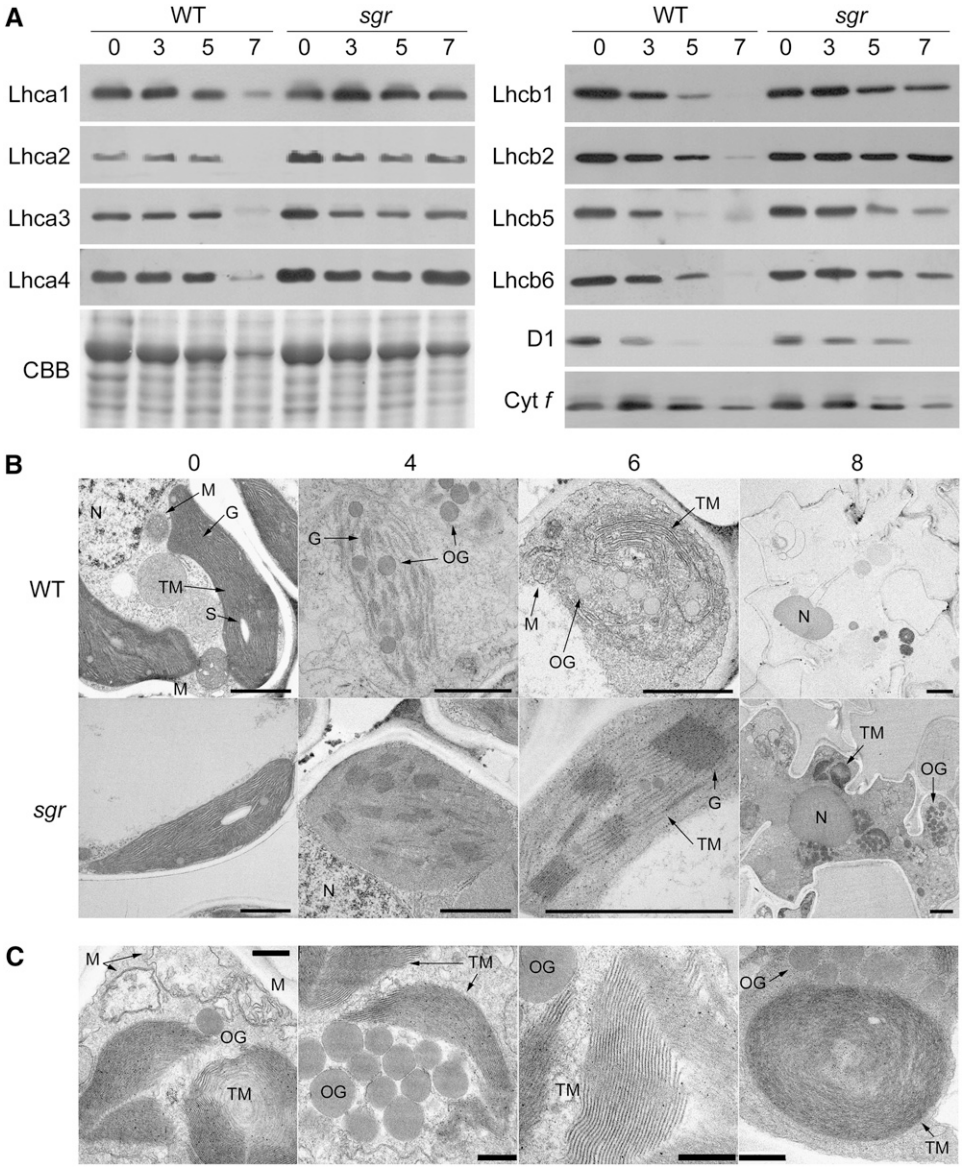

Figure 3. Immunoblot and Transmission Electron Microscopy Analyses of *sgr*.

(A) Abundance of chloroplast thylakoid proteins in leaves of the wild type and *sgr* during dark-induced senescence. One-month-old plants were excised, placed in moistened plastic bags, and incubated in complete darkness at 30°C for 8 d. Each lane contained 5 μg of total protein from leaf tissue. LHCPI, LHCPII, D1, and cytochrome *f* (Cyt *f*) were detected by immunoblotting using their specific antibodies, and then the membrane was stained by Coomassie Brilliant Blue (CBB) after Lhca4 detection. The immunoblotting was repeated at least twice with similar results. Numbers indicate DAD. The wild type was parental *japonica* cv Hwacheong-*wx*.

(B) Morphological changes in the chloroplasts of mesophyll cells in the wild type and *sgr* during dark-induced senescence. For each genotype, 20 1-month-old rice plants were used for transmission electron microscopy analysis. All green leaves were detached and incubated in complete darkness as described for **(A)**. Two to three leaves were collected at each DAD, and four to five samples were prepared from each leaf. Finally, 10 to 12 samples at each DAD were prepared for transmission electron microscopy analysis. At least three well-cut sections of each sample were used to examine the chloroplast structures. We examined 10 cells in each section and photographed the chloroplast structures that were constantly present in >7 cells. Numbers indicate DAD. G, granum; N, nucleus; OG, osmiophilic plastoglobuli; S, starch granule; TM, thylakoid membrane. Bars = 1 μm.

(C) Persistence of loose and unstacked thylakoid membranes in mesophyll cells of *sgr* at 8 DAD in **(B)**. Bars = 0.2 μm.

degree from that in the wild type (Figure 3B). The successive decomposition of chloroplast components took place in the wild type, while the stacked granum structures were maintained in *sgr* until 6 DAD. All of the chloroplast components were completely decomposed in the wild type at 8 DAD. In *sgr*, however, loose and unstacked thylakoid membranes persisted with a few osmiophilic plastoglobuli (Figures 3B and 3C). These results suggest that *sgr* has the same senescence defects as reported previously for other nonfunctional type C stay-green mutants. Thus, we conclude that leaf stay-greenness of *sgr* is mainly associated with a failure in the disassembling mechanism of the intact LHCP complexes in the thylakoid membranes, which is a prerequisite process for the degradation of Chls and Chl-free LHCPs during senescence (White and Green, 1987; Matile et al., 1999; Thomas and Howarth, 2000; Hörtensteiner and Feller, 2002; Thomas et al., 2002).

Identification of a Rice *Sgr* Gene Encoding a Function-Unknown Protein

We isolated the rice *Sgr* gene by a map-based cloning method. The single-recessive *sgr* locus was previously mapped on the long arm of chromosome 9 within 3.9 centimorgan (cM) between two restriction fragment length polymorphism (RFLP) markers, RG662 and C482 (Cha et al., 2002). With simple sequence repeat (SSR) and RFLP markers, *sgr* was further mapped within 0.6 cM between RM3636 (SSR) and E10960 (RFLP; *Eco*RI) using 305 F2 plants (Figure 4A). With an additional 860 F2 plants, 40 recombinants were isolated between RM3636 and RM1553 (Figure 4B). To make a fine physical map, several PCR-based markers, such as SSRs, cleaved amplified polymorphic sequences (CAPS), and amplified fragment length polymorphisms, were developed by aligning *japonica* and *indica* genomic DNA sequences between RM3636 in a rice PAC clone AP005314 (GenBank accession number) and E10960 in AP005092 (see Supplemental Table 1 online). By high-resolution genetic mapping, *sgr* was located within a 4.3-kb genomic region between a CAPS marker at 33.9 kb (AP5314-33.9-CAPS) and a SSR marker at 38.2 kb (AP5314-38.2-SSR) in AP005314 (Figure 4B). This region includes only one expressed gene (LOC_Os09g36200) that comprises three exons (Figure 3C). It encodes a 274–amino acid protein (30.8 kD) with a putative chloroplast signal peptide at the N terminus and no biological function (Figure 4D). In *sgr*, a single-base change from guanine to adenine was found in the second exon, which causes a Val-to-Met amino acid substitution (Figures 4C and 4D). Although there is no known domain or motif in Sgr, *Sgr* homologs identified from monocot (barley [*Hordeum vulgare*], maize, *Sorghum*, and *Zoysia*) and dicot (soybean, tomato, and *Arabidopsis*) plants showed that their protein sequences are highly conserved (see Supplemental Figure 1 online). A BLAST search and DNA gel blot analysis revealed that *Sgr* exists as a single copy in the rice genome (Figure 3E).

Sgr Is a Senescence-Associated Gene Encoding a Chloroplast Protein

In agreement with the senescence defect of *sgr*, RNA and protein gel blot analyses show that *Sgr* transcription is highly induced in response to the onset of senescence, and its protein level is increased when the leaf color changes from green to yellow (Figure 4F, left). A missense mutation in *sgr* did not affect the transcription, translation, or stabilities of mRNA and protein in senescing leaves (Figure 4F, right). *Sgr* transcripts were also detected in both newly developing and mature leaves by RT-PCR, indicating that *Sgr* is constitutively expressed at a low level during leaf development. *Sgr* transcription was suppressed by the exogenous application of a senescence-inhibiting cytokinin precursor, 6-benzyladenine (Figure 4G). These results indicate that *Sgr* is a senescence-associated gene (SAG) that is typically upregulated during senescence (Buchanan-Wollaston, 1997; Nam, 1997).

All of the Sgr homologs were predicted to have chloroplast-transit amino acids at their N termini (see Supplemental Figure 1 online). To investigate the subcellular localization of Sgr, we made a chimeric gene with full-length *Sgr* fused to the green fluorescent protein gene (*GFP*) driven by the cauliflower mosaic virus *35S* promoter (*Pro$_{35S}$:Sgr-GFP*) in the pCAMLA vector, a derivative of pCAMBIA 1300 (Lee et al., 2005). We used a transient expression assay in which we introduced *Pro$_{35S}$:Sgr-GFP* into protoplasts of *Arabidopsis* and showed that the green fluorescence by GFP colocalized with the red autofluorescence of Chls, indicating that Sgr is a chloroplast protein (see Supplemental Figure 2 online).

Sgr Overexpression Accelerates Chl Degradation in Developing Leaves

To investigate the function of Sgr in Chl degradation and test whether *Sgr* expression can induce leaf yellowing in the *sgr* background, we introduced *Pro$_{35S}$:Sgr-GFP* into the calli generated from the mature seed embryos of *sgr*, as described previously (Jeon et al., 2000). Interestingly, the transgenic rice plants that regenerated from the transformed calli of *sgr* exhibited three typical color variations in the developing leaves: green, mosaic, and yellowish-brown (Figure 5A). The transgenic rice that produced green leaves were false-positives, as determined by RT-PCR (Figure 5A, plant 2), and contained only a hygromycin-resistant *hpt* selectable marker gene but not the *Sgr-GFP* transgene (Figure 5B, lane 2). RT-PCR showed that the yellowish-brown transgenic rice accumulates the *Sgr-GFP* transcripts at higher levels than the mosaic-colored transgenic rice (Figure 5B, lanes 3 and 4), suggesting that Chl degradation is regulated by *Sgr* at the transcriptional level. Confocal microscopy analysis showed that Chls are almost absent in the chloroplasts accumulating the Sgr-GFP fusion in the yellowish-brown leaf tissues (Figure 5C), indicating that ectopic accumulation of Sgr accelerates Chl degradation even in the chloroplasts of developing leaves. After transplanting all of the transgenic rice seedlings into the soil in the growth chamber, we were only able to obtain one mature plant from the mosaic-colored rice (Figure 5A, plant 3); the others did not survive, presumably due to reduced vigor. As shown in Figure 5D, the green leaves produced at emergence in the transgenic mosaic plant progressively turned yellowish-brown as the plant grew.

Notably, the yellowish-brown leaves in the transgenic plants resembled a naturally senescent leaf phenotype. To determine

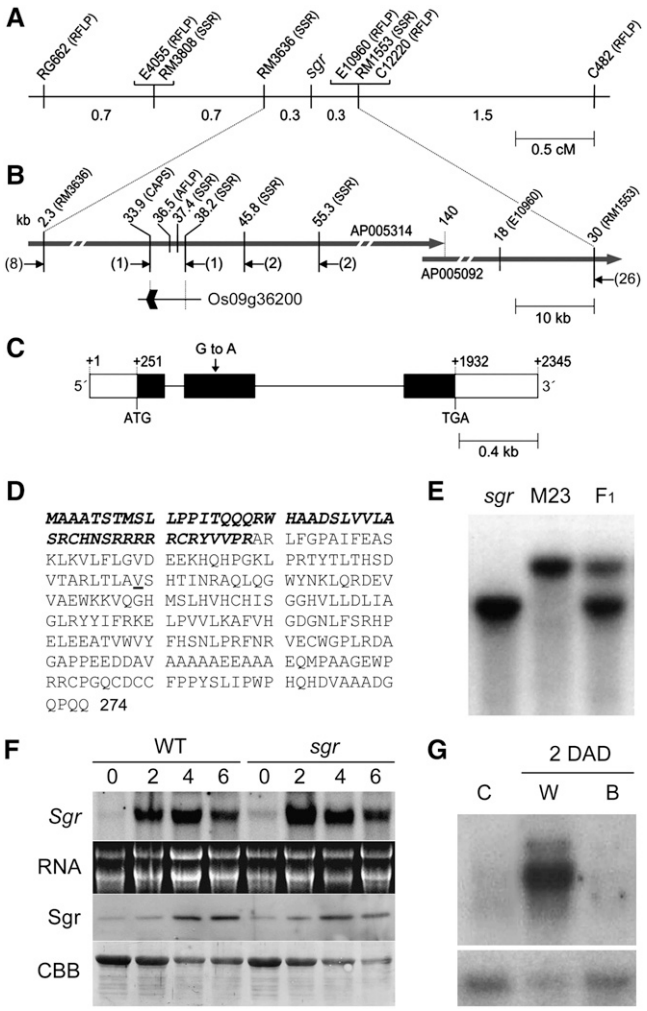

Figure 4. Map-Based Cloning and Characterization of *Sgr*.

(A) Genetic mapping of *sgr* using RFLP and SSR markers on chromosome 9.

(B) Physical mapping of *sgr* using PCR-based markers. Numbers in parentheses indicate the number of recombinant F2 individuals.

(C) Schematic representation of *Sgr* structure and the *sgr* mutation position. White and black boxes represent untranslated regions and exons, respectively. Thin lines indicate introns. The predicted translation start (ATG) and stop (TGA) sites and the nucleotide transition from guanine (G) to adenine (A) in *sgr* are indicated.

(D) Deduced amino acid sequence of Sgr. The chloroplast signal amino acids predicted by ChloroP and TargetP (Emanuelsson et al., 1999, 2000) are indicated in italicized boldface letters. A missense mutation (V99M) in *sgr* is underlined.

(E) DNA gel blot analysis with *Sgr* cDNA probe. Genomic DNAs from the mapping parent Milyang23 (M23; wild type), *sgr*, and F1 hybrid were digested with *Eco*RI.

(F) Abundance of *Sgr* mRNA and Sgr protein in leaves of the wild type and *sgr* during dark-induced senescence. One-month-old rice plants were excised, placed in moistened plastic bags, and incubated in complete darkness at 30°C for 6 d. Five micrograms of total RNA and 10 μg of total soluble protein from the leaves were loaded in each lane for RNA and protein gel blot analyses. The molecular masses of *Sgr* mRNA and Sgr protein are ~1.6 kb and 22 kD, respectively. The radiolabeled *Sgr* cDNA and the affinity-purified anti-Sgr antibody were used for probes. Because there was no available Sgr-null mutant in rice, anti-Sgr antibody specificity was determined by the antigen blocking method (see Methods). Both preimmune serum and antigen-neutralized antibody were used to examine antibody specificity and revealed that no band was detected at 22 kD. This indicates that the affinity-purified anti-Sgr antibody is specific enough to detect native Sgr in total soluble protein fractions. Numbers indicate DAD. The wild type was parental *japonica* cv Hwacheong-*wx*. CBB, Coomassie Brilliant Blue.

(G) Cytokinin effect on *Sgr* expression during dark-induced senescence. One-month-old wild-type (Hwacheong-*wx*) leaves were detached and floated on distilled water (W) or 100 μM 6-benzyladenine (B) as a cytokinin precursor and then incubated in complete darkness for 2 d. Five micrograms of total RNA was loaded in each lane. The abundance of *Sgr* transcripts (top panel) was shown based on the levels 18S rRNA (bottom panel). C indicates nontreated leaves as a negative control.

whether accelerated Chl degradation by *Sgr-GFP* overexpression induces precocious senescence in the developing leaves, we preliminarily tested the gene expression of four SAGs (*Osl2*, *Osl57*, *Osl259*, and *Osh69*; Lee et al., 2001) in the dark-induced senescing leaves of wild-type plants (see Supplemental Figure 3 online). Based on the results, *Osh69* was chosen as a senescence marker and its expression was examined in transgenic rice. *Osh69* expression was highly induced in the yellowish-brown leaves (Figure 5B, lane 4), indicating that senescence was induced in the transgenic plants. These results show that *Sgr* overexpression accelerates Chl degradation, leading to the induction of precocious senescence in the developing leaves.

Arabidopsis pao-1 and *acd1-20* Mutants Have Reduced Expression of *Sgr* Homologs during Dark-Induced, Detached Leaf Senescence

The *Arabidopsis* genome contains two *Sgr* homologs, designated *STAYGREEN1* (*SGN1*; At4g22920) and *SGN2* (At4g11910) (see Supplemental Figure 1B online), whose transcript levels are increased during dark-induced, detached leaf senescence (Figure 6A). In *Arabidopsis* leaf 4, the SGN proteins are present at basal levels during leaf development. Their levels were increased with leaf aging and reached their peak when the leaf color turned completely yellow during natural senescence (Figure 6B). Lack of PaO activity caused high accumulation of Chls and Pheide *a* in the detached leaves of *pao1* and *acd1-20* mutants during dark-induced senescence, resulting in a stay-green phenotype (Figures 6C to 6E). To determine how a deficiency of PaO activity is correlated with the substantial retention of Chls and LHCPII in *Arabidopsis* and maize during dark-induced senescence (Pružinská et al., 2003, 2005), we examined *SGN* expression in the dark-induced senescing leaves of *pao1* and *acd1-20*. RNA and protein gel blot analyses revealed that during dark-induced senescence, both *pao1* and *acd1-20* have much reduced expression of *SGN* genes (Figure 6F); therefore, SGN proteins are not detectable in their senescing leaves (Figure 6G). These results indicate that a high level of Pheide *a* or a deficiency of PaO activity negatively affects *SGN* expression, resulting in a stay-green phenotype that is similar to that of the *sgr* mutant under dark-induced senescence conditions (Figure 1C).

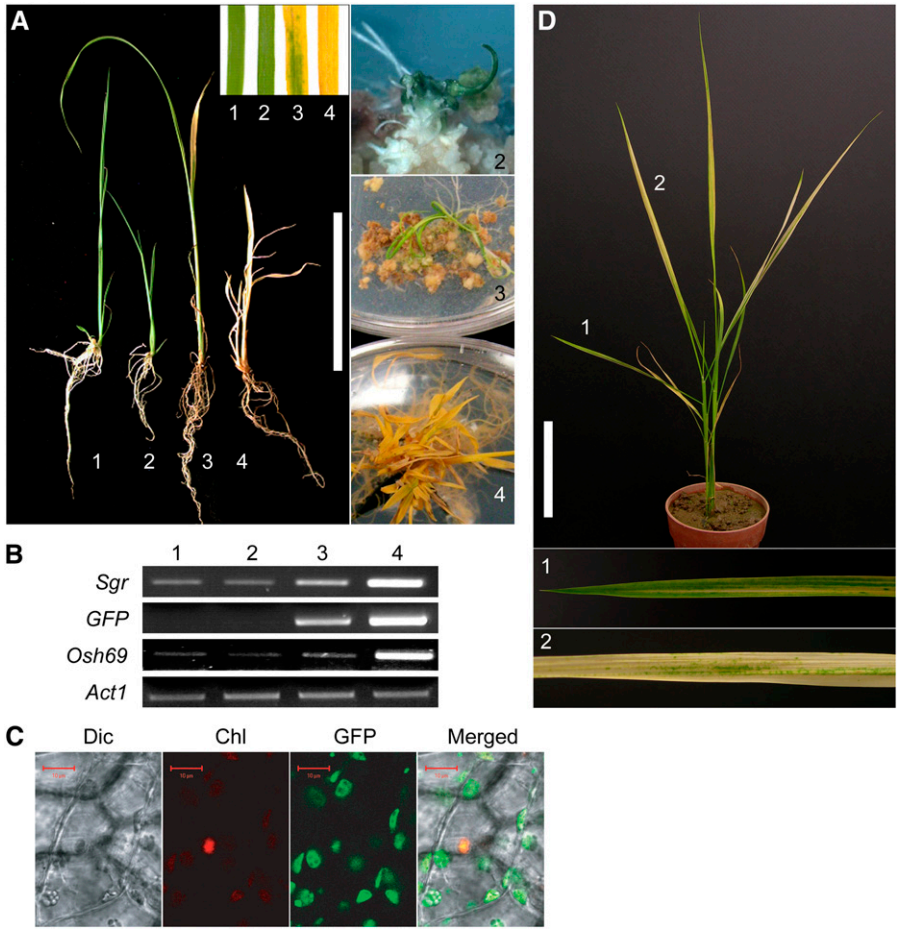

Figure 5. Overexpression of *Sgr-GFP* in the *sgr* Background.

(A) Leaf colors of transgenic rice plants regenerated from the calli of *sgr* mutant embryos transformed with Pro_{35S}:*Sgr-GFP*. Plant 1, nontransgenic wild-type plant (Hwacheong-*wx*); plants 2 to 4, transgenic plants exhibiting green (plant 2), mosaic (plant 3), and yellowish-brown (plant 4) phenotypes. Bar = 10 cm.

(B) Abundance of the *Sgr-GFP* transcripts in **(A)** by semiquantitative RT-PCR. The presence of *GFP* transcripts indicates true transformants, and *Osh69* expression was used as a senescence marker (see Supplemental Figure 3 and Supplemental Table 1 online). *Actin1* (*Act1*) was used as a loading control.

(C) Chl degradation in the chloroplasts of yellowish-brown leaves in **(A)** (plant 4). Dic, differential interference contrast. Bars = 10 μm.

(D) A mature plant phenotype that survived from the transgenic mosaic seedlings in **(A)** (plant 3).

Sgr Does Not Have Chl Binding or Chlorophyllase Activity

To examine whether Sgr has Chl binding activity as a Chl carrier (Matile et al., 1997, 1999; Hörtensteiner and Matile, 2004), we prepared a recombinant ΔSgr protein fused with the maltose binding protein (MBP), MBP-ΔSgr fusion (Δ indicates deletion of the N-terminal chloroplast-transit 48 amino acids). The Chl binding activity of Sgr was examined by mixing the purified MBP-ΔSgr fusion with spinach (*Spinacia oleracea*) Chls in the Chl binding buffer and then applying the mixtures to native polyacrylamide gels as described previously (Satoh et al., 1998). The purified MBP was used as a negative control and the MBP-ΔWSCP fusion (Satoh et al., 1998) was used as a positive control. The Chl fluorescence band was observed only with the MBP-ΔWSCP fusion under long-waved UV light (see Supplemental Figure 4 online), suggesting that Sgr has no Chl binding activity in vitro.

To determine whether Sgr has chlorophyllase activity, we prepared the glutathione *S*-transferase (GST)–Sgr fusion with a GST-At CLH2 fusion as a positive control because we had no information on rice chlorophyllase genes (see Supplemental Figure 5 online). When the purified fusion proteins were added to a solution containing Chls, the GST-Sgr fusion was not capable of converting Chls into Chlides, whereas the GST-At CLH2 fusion produced Chlides as described previously (Tsuchiya et al., 1999; Benedetti and Arruda, 2002). The reaction mixture with the GST-At CLH2 and GST-Sgr fusions showed the same rate of Chlide production as that containing only the GST-At CLH2 fusion, indicating that there is no synergistic effect of Sgr on the chlorophyllase activity of At CLH2. Together, these in vitro results

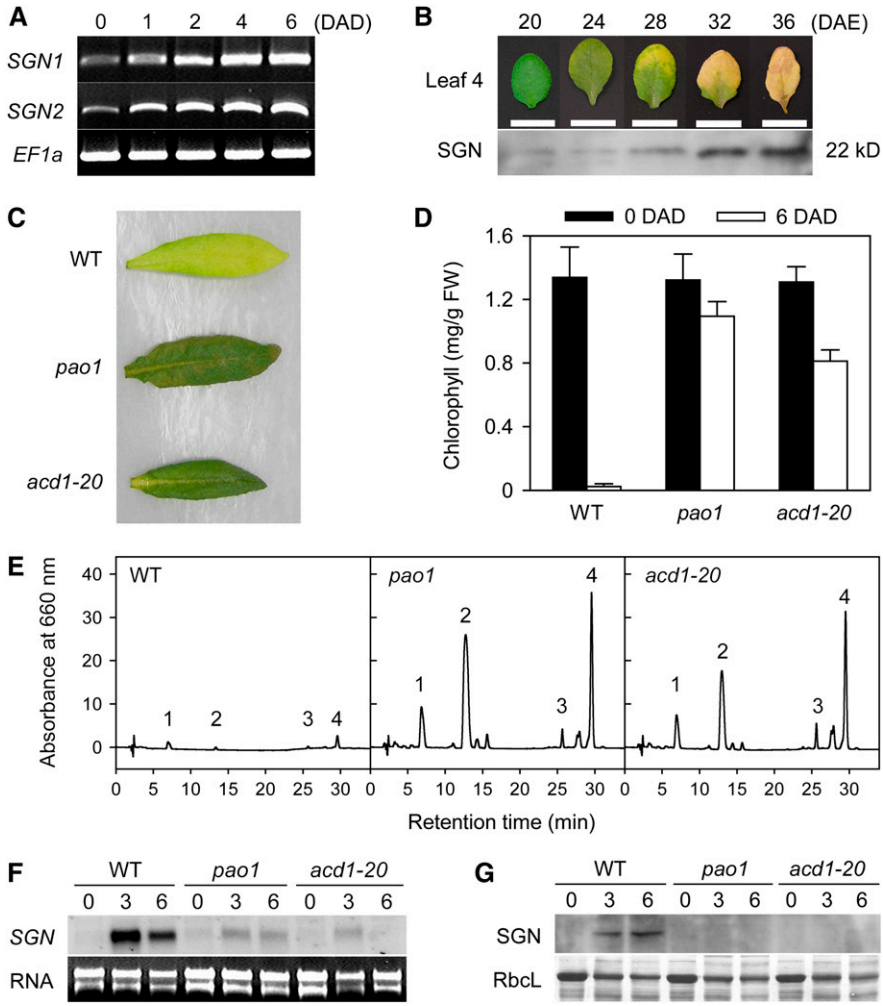

Figure 6. Expression Patterns of *Sgr* Homologs in *Arabidopsis* Wild Type and PaO-Impaired Mutants during Leaf Senescence.

(A) Abundance of *SGN1* (At4g22920) and *SGN2* (At4g11910) mRNAs during dark-induced, detached leaf senescence in *Arabidopsis. Arabidopsis* (Columbia-0) plants were grown at constant 22°C under cool-white fluorescent light (100 $\mu mol \cdot m^{-2} \cdot s^{-1}$) in long days (16 h of light/8 h of dark) in the growth chamber. Rosette leaves (leaves 5 to 7) were detached at bolting, placed on Parafilm, and floated in distilled water on Petri plates. They were stored in complete darkness at 22°C. *ELONGATION FACTOR1a* (*EF1a*) was used as a loading control. Primer information for RT-PCR is listed in Supplemental Table 1 online.

(B) SGN accumulation in *Arabidopsis* wild-type leaf 4 during natural senescence. *Arabidopsis* (Columbia-0) plants were grown under the same condition described for **(A)**. Rosette leaf 4 was sampled every 4 d from 20 d after emergence (DAE) until it turned completely yellow. Anti-Sgr antibody was used for immunoblot analysis. Twenty micrograms of total soluble protein extracted from three leaves was loaded in each lane.

(C) Stay-green leaf phenotypes of *pao1* and *acd1-20* at 6 DAD. Plants were grown under the same conditions described for **(A)** except that continuous light was used. Green rosette leaves (leaves 5 to 7) of 3-week-old plants were detached from each genotype, and dark treatment was the same as in **(A)**. Leaf 7 of each genotype was photographed at 6 DAD. This analysis was performed at least three times with the same results. The wild type was Columbia-0.

(D) Chl retention in *pao1* and *acd1-20* during dark-induced senescence. Leaf samples in **(C)** were used. Green rosette leaves (leaves 5 to 7) of 3-week-old plants were detached and placed in complete darkness as in **(A)**. Mean and SD values were obtained from three replications. FW, fresh weight.

(E) HPLC results of Chls and Chl catabolites in detached leaves of the wild type, *pao1*, and *acd1-20* at 6 DAD. This analysis was performed three times with similar results. Peak 1, Chlide *a*; peak 2, Pheide *a*; peak 3, Chl *b*; peak 4, Chl *a*.

(F) Reduced expression of *SGN* genes in *pao1* and *acd1-20* during dark-induced, detached leaf senescence. Five micrograms of total RNA extracted from three leaves (leaves 5 to 7) in **(C)** was loaded in each lane. Due to high sequence similarity between *SGN1* and *SGN2* cDNA sequences, the full-length *SGN2* cDNA was used as a probe. Numbers indicate DAD. This analysis was performed twice with similar results.

(G) No accumulation of SGN proteins in *pao1* and *acd1-20* during dark-induced, detached leaf senescence. Ten micrograms of total soluble RNA extracted from three leaves (leaves 5 to 7) in **(C)** was loaded in each lane. Anti-Sgr antibody was used for immunoblotting, and then the membrane was stained with Coomassie Brilliant Blue. This analysis was performed at least three times with the same results. RbcL, ribulose-1,5-bis-phosphate carboxylase/oxygenase large subunit.

strongly suggest that Sgr does not have Chl binding or chlorophyllase activity.

Transient Overexpression of *Sgr* Activates the Degradation of Chls and LHCPs during Leaf Development in *Nicotiana benthamiana*

All of our results suggested that Sgr plays an important role in triggering the disassembly of the LHCP complexes in senescing chloroplasts. In this respect, the yellowish-brown leaf phenotype of transgenic rice (Figure 5A, plant 4) suggests that catabolic enzymes and proteases for the degradation of Chls and Chl-free LHCPs may be constitutively present and/or rapidly induced in the developing leaf cells when *Sgr* is expressed. Furthermore, the fact that Chl degradation is not completely blocked in the senescing *sgr* leaves (Figure 1D) suggests that the mutant protein in *sgr* (sgr [V99M]) may be partially active.

To verify these assumptions, we performed the transient overexpression assay by infiltrating leaves of *N. benthamiana* at three different developmental stages with the recombinant agrobacteria containing the Pro_{35S}*:Sgr* or Pro_{35S}*:sgr* construct (Figures 7A and 7B). We found that the green leaf spots infiltrated by Pro_{35S}*:Sgr* began to turn yellow at 3 d after infiltration and continued to spread widely, but those infiltrated by Pro_{35S}*:sgr* or negative controls did not turn yellow (see Supplemental Figures 6A and 6B online). These findings demonstrate that transient overexpression of *Sgr* can induce Chl degradation in *N. benthamiana* much like in transgenic rice constitutively expressing the *Sgr-GFP* (Figure 5A, plant 4). Protein analysis revealed that progressive degradation of LHCPI and LHCPII and total soluble protein fractions occurred in leaves accumulating Sgr but not in those accumulating sgr (V99M) (Figure 7C) or GFP (negative control; see Supplemental Figure 6C online). These results suggests that the missense mutation in sgr (V99M) may lead to a loss of function and that the transient accumulation of Sgr is enough to cause LHCP disassembly in a dicot plant, resulting in the degradation of Chls and Chl-free LHCPs in the presence and/or by the rapid induction of catabolic enzymes and proteases in the infiltrated regions of presenescent *N. benthamiana* leaves.

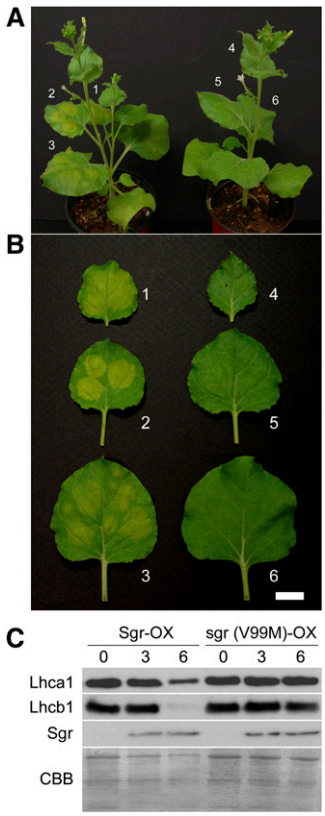

Figure 7. Transient Overexpression of Sgr and sgr (V99M) in *N. benthamiana*.

(A) Plant phenotypes of *N. benthamiana* infiltrated by recombinant agrobacteria containing Pro_{35S}*:Sgr* (left plant; 1 to 3) or Pro_{35S}*:sgr* (right plant; 4 to 6) in the pMBP-1 vector at 6 d after infiltration. Four of the 1-month-old plants were used for each infiltration and showed similar results.
(B) Infiltrated leaf phenotypes of *N. benthamiana* in **(A)**. Bar = 2 cm.
(C) Changes in the abundance of LHCP subunits in infiltrated leaves of *N. benthamiana* from the accumulation of Sgr (leaf 1 in **[B]**) or sgr (V99M) (leaf 4 in **[B]**). Anti-Lhca1, anti-Lhcb1, and anti-Sgr antibodies were used for immunoblot analyses. The membrane was stained with Coomassie Brilliant Blue (CBB) after Lhca1 immunodetection. The molecular masses of Lhca1, Lhcb1, and Sgr are ~22, 28, and 22 kD, respectively. Each lane represents the protein concentration of a 1-cm leaf disc (see Methods). This analysis was repeated twice with similar results. Numbers indicate days after infiltration. Day 0 indicates noninfiltrated leaf discs. OX, overexpression.

Sgr Interacts with LHCPII in Vivo

As inferred from the above results, it can be assumed that Sgr is directly involved in the destabilizing mechanism of the intact LHCP complexes during leaf senescence. Thus, to determine the molecular function of Sgr, we examined whether Sgr interacts with the LHCP complexes or other chloroplast proteins. For a preliminary experiment, we performed an in vitro pull-down assay by mixing the MBP-ΔSgr fusion with total soluble proteins extracted from mature leaves of rice. In the MBP pull-down, the MBP-ΔSgr fusion was copurified with both LHCPI and LHCPII (Figure 8A) but not with other thylakoid proteins (D1 and cytochrome *f*) or a stromal protein (RbcL), indicating that Sgr has specific affinity for LHCPI and LHCPII in our in vitro binding conditions.

To verify this interaction, we performed an in vivo pull-down assay with the leaves of *N. benthamiana* transiently overexpressing the Sgr-GST and sgr (V99M)-GFP fusions. At 6 d after infiltration, leaf yellowing occurred in *N. benthamiana* that was infiltrated by Pro_{35S}*:Sgr-GST* but not by Pro_{35S}*:sgr-GFP*, Pro_{35S}*:GFP*, or Pro_{35S}*:GST* (data not shown), indicating that the Sgr-GST fusion is functional and that sgr (V99M)-GFP is nonfunctional in *N. benthamiana*. Accumulation of the Sgr-GST, sgr (V99M)-GFP, GST, and GFP proteins was verified by immunoblot analysis with total soluble protein fractions extracted from the leaves at 4 d after infiltration (Figure 8B). The GST and GFP pull-down results revealed that the Sgr-GST and sgr (V99M)-GFP fusions were copurified with LHCPII (Figure 8C) but not with LHCPI or other chloroplast proteins such as D1, cytochrome *f*,

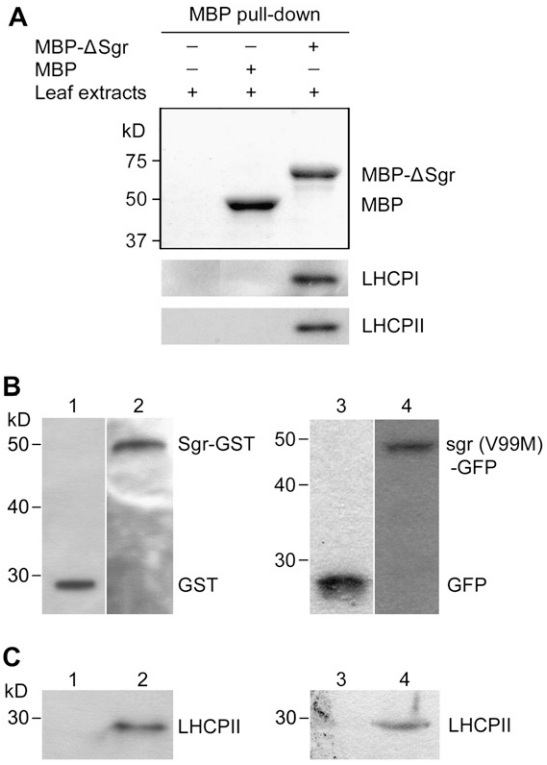

Figure 8. Sgr Interacts with LHCPII.

(A) Sgr has specific affinity for LHCPI and LHCPII in vitro. Each sample was pulled down using amylose agarose resin (see Methods). LHCPI and LHCPII were detected by immunoblot using anti-Lhca4 and anti-Lhcb2 antibodies. The membrane was then stained with Coomassie Brilliant Blue (top panel). The total soluble protein fraction from green leaves of 1-month-old rice plants was used for the in vitro pull-down assay. The in vitro pull-down experiments were repeated three times with the same results.

(B) Transient overexpression of Sgr-GST, GST, sgr (V99M)-GFP, and GFP in leaves of *N. benthamiana*. Pro_{35S}*:GST* (lane 1) or Pro_{35S}*:Sgr-GST* (lane 2) in the pMBP-1 vector, or Pro_{35S}*:GFP* (lane 3) or Pro_{35S}*:sgr-GFP* (lane 4) in the pCAMLA vector, was infiltrated into green leaves of 1-month-old *N. benthamiana* plants as in Figure 7. In vivo protein expression was verified with the infiltrated leaves at 4 d after infiltration by immunoblot using anti-GST (left panel) and anti-GFP (right panel) antibodies.

(C) Sgr and sgr (V99M) interact with LHCPII in *N. benthamiana*. From the total soluble protein fractions extracted from the infiltrated leaves in **(B)**, GST (lane 1) and Sgr-GST fusion (lane 2) were pulled down using glutathione Sepharose beads (left panel), and GFP (lane 3) and sgr (V99M)-GFP fusion (lane 4) were immunoprecipitated using anti-GFP antibody (right panel) (see Methods). LHCPII was detected by immunoblotting using anti-Lhcb1 antibody. LHCPI was not detected with any of the four anti-Lhca antibodies. The in vivo GST pull-down and GFP coimmunoprecipitation assays were performed at least twice with the same results.

and RbcL. GFP and GST (negative controls) did not react with any of the antibodies by immunoblotting. These results indicate that Sgr binds directly to the intact LHCPII complexes on the stromal side of thylakoid membranes of the chloroplasts and that the missense mutation in sgr (V99M) does not affect the binding activity to LHCPII in vivo.

DISCUSSION

Many reports have shown that Chl catabolism is highly regulated by genetic programs during development and senescence in plants. For this reason, the stay-green mutants identified from several plant species have long been investigated to elucidate the unknown regulatory mechanism of Chl degradation. Here, we report the nonfunctional type C stay-green *Sgr* genes in rice and other plants and the regulatory function of Sgr protein during leaf senescence. Our results show that *Sgr* is a senescence-associated gene encoding a novel chloroplast protein that interacts with LHCPII in the chloroplasts. Thus, we propose that the Sgr-LHCPII complexes are formed on the stromal side of thylakoid membranes in order to trigger LHCPII destabilization for the degradation of Chls and Chl-free LHCPII subunits in senescing leaves.

Sgr Encodes a Novel Chloroplast Protein That Activates Chl Degradation

We show that *sgr* maintains leaf greenness during natural and dark-induced senescence because Chl degradation is much slower (Figure 1D) (Cha et al., 2002). During dark-induced senescence, green Chl catabolites, Chlide *a* and Pheide *a*, accumulate in the senescent leaves of *sgr* to higher levels than in wild-type leaves (Figure 2). In this respect, we conclude that the rice *sgr* mutant has the same characteristics as other nonfunctional type C stay-green mutants from *F. pratensis*, *P. vulgaris*, tomato, and pepper, which also accumulate significant amounts of Chlide *a* and/or Pheide *a* in their senescing leaves (Vicentini et al., 1995; Fang et al., 1998; Akhtar et al., 1999; Roca and Mínguez-Mosquera, 2006).

Sgr is a nuclear gene encoding a chloroplast protein, and its homologs exist as either single or duplicate genes in higher plants but not in photosynthetic bacteria or other organisms (see Supplemental Figure 1 online). The amino acid sequences of Sgr proteins show high sequence homology, suggesting that these genes have been highly conserved during plant evolution in order to maintain their unique function in Chl catabolism. *Sgr* is a senescence-associated gene (Figure 4F), which is in agreement with a previous report that new protein synthesis in the cytoplasm is required for Chl degradation even in the presence of high chlorophyllase activity in senescing leaves (Thomas et al., 1989). Furthermore, the subcellular localization of the Sgr-GFP fusion in chloroplasts (see Supplemental Figure 2 online) strongly supports the direct effect of Sgr on Chl degradation during senescence. Interestingly, microarray data from the Genevestigator database (https://www.genevestigator.ethz.ch/; Zimmermann et al., 2004) show that *SGN1* (At4g22920) is highly expressed not only in senescing leaves but also in floral organs, during seed maturation, under nitrogen-deficient and osmotic stresses, and by pathogen attack and abscisic acid application. This finding indicates that *Sgr* transcription is highly induced not only by the onset of senescence (Figures 4F and 6A) but also by developmental signals and environmental stresses, possibly in order to prevent Chl accumulation or activate Chl catabolism during development.

Sgr is constitutively expressed at low levels; therefore, low amounts of Sgr are detected during leaf development (Figures

4F, 5B, and 6B). In *Arabidopsis*, both *PAO* and PaO are also constitutively expressed at low levels during development, and their levels are rapidly increased during senescence (Pružinská et al., 2005). This suggests that massive breakdown of Chls during senescence is required for the upregulation of *Sgr* and *PAO*. Armstead et al. (2007) recently reported that RNA interference silencing of At4g22920 in transgenic *Arabidopsis* plants leads to a stay-green phenotype during dark-induced, detached leaf senescence. Furthermore, stay-green pea (*Pisum sativum*) plants have much reduced expression of the pea *Sgr* homolog in senescing leaves than do wild-type plants, indicating that Chl retention in both the stay-green pea mutant and RNA interference–silenced stay-green *Arabidopsis* results from the deficiency of Sgr activity. Here, we show that the substantial retention of Chls in the dark-induced senescing leaves of *Arabidopsis pao1* and *acd1-20* mutants is closely associated with the reduced expression of *Sgr* homologs, *SGN1* and *SGN2* (Figure 6F). This finding strongly suggests that either an increase of Pheide *a* or a decrease of PaO activity in the chloroplasts participates in the negative feedback regulation of plastid to nucleus to repress *SGN* genes at the transcription level; therefore, a stay-green phenotype can be seen in the dark-induced senescent leaves of *Arabidopsis* PaO-impaired mutants.

Sgr Interacts with LHCPII for LHCP Destabilization in Senescing Chloroplasts

In the chloroplasts, the LHCP complexes become stabilized via the integration of Chls, resulting in the inhibition of LHCP degradation, and the thylakoid membranes are not disassembled until after the degradation of both Chls and LHCPs (White and Green, 1987; Hörtensteiner and Feller, 2002; Hörtensteiner and Matile, 2004). In other words, the dissociation of Chls from the LHCP complexes is a prerequisite for the degradation of Chls, LHCPs, and thylakoid membranes in senescing leaf cells. Chlorophyllase activity is present not only in senescing leaves or ripening fruits but also in developing and mature leaves or developing fruits (Tang et al., 2004). In addition, At FtsH6, a protease interacting with LHCPII, is constitutively expressed in the chloroplast thylakoid membranes and is involved in LHCPII degradation during senescence as well as during high-light acclimation in *Arabidopsis* (Garcia-Lorenzo et al., 2005; Żelisko et al., 2005). Thus, the latency of chlorophyllases and At FtsH6 in green leaves suggests that they become activated to degrade Chls and Chl-free LHCPs after the LHCP destabilization that is impaired in *sgr* during senescence (Figure 3A). In this respect, our data strongly support the notion that Sgr acts as a key regulator for the disassembly of intact LHCP complexes in the chloroplasts.

We showed that Sgr has specific affinity for rice LHCPI and LHCPII in vitro (Figure 8A) and confirmed that Sgr binds directly to LHCPII in vivo (Figure 8C) through transient overexpression of the Sgr-GST fusion in the leaves of *N. benthamiana*. These in vitro results suggest that Sgr does not have Chl binding or chlorophyllase activity, suggesting that Sgr is not involved directly in the Chl catabolic pathway. Moreover, our in vitro and in vivo pull-down assays showed no evidence that Sgr is capable of interacting with other thylakoid proteins, D1 and cytochrome *f*, or a major stromal protein RbcL, although these negative results are not always true and should be further determined. Based on all of the results in this study, we propose a hypothetical molecular mechanism to explain how Sgr regulates the degradation of Chls and LHCPs during senescence. The senescence-induced Sgr localizes to the chloroplasts and binds to the LHCPII complex, resulting in the formation of the Sgr-LHCPII complexes on the stromal side of the thylakoid membranes. In the presence of catabolic enzymes and/or other interacting proteins in senescing leaf cells, Sgr-LHCPII complex formation destabilizes the intact LHCPII complex bound to the thylakoid membranes, which may facilitate catabolic enzymes and proteases to access their substrates directly. The missense mutation of sgr (V99M) does not affect the in vivo interaction of LHCPII (Figure 8C), indicating that the formation of the sgr (V99M)-LHCPII complex in the thylakoid membranes does not induce LHCP disassembly. Thus, we speculate that an amino acid substitution in sgr (V99M) may disrupt either an enzymatic activity or a binding activity to other regulatory factor(s) that is essential for LHCPII disassembly. In addition, since LHCPI degradation is also impaired in *sgr* (Figure 3A), it remains to be determined whether the Sgr-LHCPII complexes affect LHCPI destabilization simultaneously or whether LHCPI degradation involves other chloroplast proteins in the presence of Sgr.

The nonfunctional type C stay-green *y* locus in *Festuca*/*Lolium* plants is syntenically equivalent to the *sgr* locus on rice chromosome 9, and indeed, the *y* mutation results from a 4-bp insertion in a homolog of *Sgr* (Armstead et al., 2006). Genetic mapping of Mendel's green pea revealed that the pea *sgr* locus was cosegregated with the green cotyledon locus in two different pea populations segregating for yellow and green cotyledon color (Armstead et al., 2007). However, the *Arabidopsis ore10* mutant shows normal degradation of LHCPI but high stability of intact LHCPII trimer and/or trimmed LHCPII aggregates in senescent leaves (Oh et al., 2000, 2003). The *ore10* locus in *Arabidopsis* was recently mapped to within 2 cM of the RCI1b locus on chromosome 5 (Oh et al., 2006), whereas two *SGN* genes are located on chromosome 4. The cytoplasmically inherited stay-green mutation in soybean, *cytG*, also retains LHCPII, but not LHCPI, during monocarpic senescence (Guiamét et al., 1991, 2002), suggesting that the degradation of LHCPI and LHCPII occurs in different metabolic pathways and that other chloroplast components must be required for LHCPII disassembly in senescing chloroplasts. Thus, future work is necessary to elucidate the nature of chloroplast proteins involved in the molecular events of LHCP disassembly. Gene cloning from other nonfunctional type C stay-green mutants as well as the identification of additional chloroplast components participating in LHCP disassembly will provide new insights into the regulatory mechanism for the degradation of Chls and Chl-free LHCPs during leaf senescence.

METHODS

Plant Materials and Preparation of the Mapping Population

The induction and isolation of *sgr* from the parental rice (*Oryza sativa*) *japonica* cv, Hwacheong-*wx*, the preparation of an F2 population by crossing *sgr* with the *indica-japonica* hybrid cv Milyang23 as a mapping parent, and the F2 genotyping by F3 test were described previously (Cha

et al., 2002). Primer information of the PCR-based markers for physical mapping is listed in Supplemental Table 1 online.

HPLC Analysis of Green Pigments

For reverse-phased HPLC analysis, the Hewlett-Packard HPLC system fitted with an automatic injector and a photodiode array detector (HP1100) was used, and the absorption of each pigment was recorded at 660 nm (Roca et al., 2004). The green pigments were separated on a 4 × 250 mm LiChrosper C18 column (Merck) using two solvents, 100% ethyl acetate and 80% methanol for a linear gradient. The injection volume was 10 μL, and the flow rate was 1 mL/min. Identification of each pigment was based on retention time and visible absorption using the pigment standards Chl *a* and Chl *b* (Sigma-Aldrich), Chlide *a* (DHI), and Pheide *a* (Tama Biochemical).

Leaf Protein Preparation and Immunoblot Analysis

For total soluble protein extraction, leaf tissues were finely ground in liquid nitrogen and homogenized with the extraction buffer (50 mM potassium phosphate, pH 7.8, 5 mM EDTA, 0.05% 2-mercaptoethanol, and 1 mM phenylmethylsulfonyl fluoride). After centrifugation, the protein concentration was determined with the Bio-Rad Protein Assay reagent. Equal amounts of protein samples were subjected to SDS-PAGE on 12% polyacrylamide gels and then transferred to a polyvinylidene difluoride (PVDF) membrane (Amersham). To examine the profiles of total soluble protein on the basis of leaf area during senescence, leaf discs (1 cm diameter) were sampled and finely ground with a plastic pestle or metal beads in liquid nitrogen in a 1.5-mL microcentrifuge tube. Tissue powder was homogenized with 0.2 mL of 6× SDS sample buffer, boiled for 5 min, and centrifuged for 30 min at 22°C with maximum speed. An equal volume of the supernatants was subjected to SDS-PAGE for immunoblot analysis. The level of each protein was examined by immunoblot analysis using the ECL system (Amersham) or nitroblue tetrazolium/5-bromo-4-chloro-3-indolyl phosphate (Pierce). Antibodies against LHCPI subunits (Lhca1, Lhca2, Lhca3, and Lhca4), LHCPII subunits (Lhcb1, Lhcb2, Lhcb5, and Lhcb6), D1, cytochrome *f*, and RbcL were purchased from AgriSera, anti-MBP and anti-GST antibodies were from Santa Cruz Biotechnology, and anti-GFP antibody was from Abcam.

Transmission Electron Microscopy Analysis of Chloroplasts

Transmission electron microscopy analysis was performed as described previously (Inada et al., 1998) with minor modifications. Segments of leaf tissues were fixed with a modified Karnovsky's fixative (2% paraformaldehyde, 2% glutaraldehyde, and 50 mM sodium cacodylate buffer, pH 7.2) and washed three times with 50 mM sodium cacodylate buffer, pH 7.2, at 4°C for 10 min. The samples were postfixed with 1% osmium tetroxide in 50 mM sodium cacodylate buffer, pH 7.2, at 4°C for 2 h, and briefly washed twice with distilled water at 25°C. Samples were en bloc stained in 0.5% uranyl acetate at 4°C for a minimum of 30 min, dehydrated in a gradient series of ethanol and propylene oxide, and finally embedded in Spurr resin. After polymerization at 70°C for 24 h, ultrathin sections were prepared with a diamond knife on an ultramicrotome (MT-X) and mounted on Formvar-coated copper grids. The sections on the grids were stained with 2% uranyl acetate for 5 min and with Reynolds' lead citrate for 2 min at 25°C and then examined with a JEM-1010 EX electron microscope (JEOL).

RNA Gel Blot and Semiquantitative RT-PCR Analyses

For RNA gel blot analysis, total RNA from leaf tissues was extracted using TRIzol reagent according to the manufacturer's protocol (Invitrogen). Total RNA was loaded onto formaldehyde gels and transferred to nylon membrane (Hybond-N^+; Amersham). The ^{32}P-labeled *Sgr* cDNA, At4g11910 cDNA, and 18S rDNA fragments were used as probes. For semiquantitative RT-PCR, total RNA was treated with a DNA-free reagent (Ambion) to remove possible contamination of genomic DNA and reverse-transcribed with oligo(dT) primer (Promega) or a gene-specific reverse primer for *18S rRNA* using the First-Strand cDNA synthesis kit (Roche). The PCR primer sets for *Sgr*, *GFP*, *hpt*, *Act1* (*Act1*), *Osl2*, *Osl57*, *Osl259*, *Osh69*, *18S rRNA*, *SGN1* (At4g22920), *SGN2* (At4g11910), and *EF1a* are listed in Supplemental Table 1 online.

Plasmid Construction for Transformation

To construct the *Pro$_{35S}$:Sgr-GFP* or *Pro$_{35S}$:sgr-GFP* fusion, the open reading frame of *Sgr* was inserted between the cauliflower mosaic virus 35S promoter (*Pro$_{35S}$*) and *GFP* (*Pro$_{35S}$-Xba*I-*Sgr* or *sgr-Bam*HI-*GFP-Sac*I) in the pCAMLA vector that was developed previously by insertion of *GFP* into the pCAMBIA 1300 vector (Lee et al., 2005). For *Pro$_{35S}$:Sgr* or *Pro$_{35S}$:sgr*, the open reading frame of *Sgr* or *sgr* was inserted into the pCAMBIA 1300 vector (*Pro$_{35S}$-Xba*I-*Sgr* or *sgr-Kpn*I). The *sgr* cDNA was amplified by RT-PCR from dark-treated leaves of *sgr* and cloned into pGemT Easy vector (Promega). For *Pro$_{35S}$:GST*, we cloned *GST* having *Bam*HI at the 5′ flanking region and *Kpn*I at the 3′ flanking region by PCR using pGEX-4T-1 vector, and it was inserted into pMBP-1 binary vector (*Pro$_{35S}$-Bam*HI-*GST-Kpn*I), a derivative of pBI121 (Yi et al., 2004). For the *Pro$_{35S}$:Sgr-GST* fusion, the open reading frame of *Sgr* was inserted in front of *GST* into the *Pro$_{35S}$:GST* vector (*Pro$_{35S}$-Xba*I-*Sgr-Bam*HI-*GST-Kpn*I). Primer information is listed in Supplemental Table 1 online.

Plasmid Construction for Fusion Protein Purification

To produce the MBP fusion protein, a truncated open reading frame of *Sgr* (*ΔSgr*, without the N-terminal chloroplast-transit 48 amino acids) was prepared by PCR using the *Sgr* cDNA and then fused downstream of the MBP-coding gene into the pMAL-c2 expression vector (New England Biolabs). The MBP-ΔSgr fusion protein was purified using amylose resin (New England Biolabs). To purify the His-tagged proteins, *ΔSgr* was inserted downstream of the His-coding gene into the pET-15b expression vector (Novagen). The His-ΔSgr fusion protein was purified using nickel-nitrilotriacetic acid agarose beads (New England Biolabs). For the preparation of GST-Sgr and GST-At CLH2 fusion proteins, *Sgr* and At *CLH2* were fused downstream of *GST* in the pGEX-4T-1 vector (Amersham) and the GST fusion proteins were purified using glutathione–Sepharose beads (Sigma-Aldrich). MBP and GST proteins were expressed and purified for negative controls. The At *CLH2* cDNA was cloned by RT-PCR using total RNA extracted from the *Arabidopsis thaliana* (Columbia ecotype) rosette leaves. These recombinant expression vectors were introduced into *Escherichia coli* cells, BL21 Codon Plus (Stratagene) or Rosetta 2(DE3) (Novagen), to produce the fusion proteins. Protein induction and purification were performed according to the manufacturers' manuals. Primer information is listed in Supplemental Table 1 online.

Production and Affinity Purification of Anti-Sgr Antibody

To produce a polyclonal anti-Sgr antibody, the His-ΔSgr fusion protein isolated from Rosetta 2(DE3) *E. coli* extracts was subjected to SDS-PAGE and then eluted from the gel after Coomassie Brilliant Blue staining for immunization. Anti-Sgr antiserum was obtained from two rabbits immunized with the gel-purified His-ΔSgr (LabFrontier). For antibody purification from antiserum, anti-Sgr antibodies were further affinity-purified by absorption to the MBP-ΔSgr fusion protein that was bound to a PVDF membrane (Amersham).

Determination of Anti-Sgr Antibody Specificity by Antigen Blocking

To examine the affinity-purified anti-Sgr antibody specificity, it was determined by competing with an excess of antigen (His-ΔSgr) as described

in a laboratory protocol (Alpha Diagnostics International; http://www.4adi.com/tech/ablock.html), since the Sgr-null mutant was not available in rice. The concentrations of the affinity-purified antibody and antigen (His-ΔSgr) were determined with the Bio-Rad Protein Assay reagent (Bio-Rad), and then the antibody was reacted with a 50-fold amount of antigen. After centrifugation, the supernatant was collected as the neutralized antibody solution. The antigen-neutralized antibody and preimmune serum were tested to determine whether they react with the native Sgr protein in total soluble protein extracted from the dark-treated rice leaves.

Subcellular Localization of the Sgr-GFP Fusion Protein

Pro_{35S}:Sgr-GFP or *Pro_{35S}:GFP* in pCAMLA vector was transfected into the protoplasts isolated from rosette leaves of *Arabidopsis* (Columbia) by the polyethylene glycol method (Gindullis and Meier, 1999). GFP fluorescence was examined with an argon ion laser at 488 nm using a confocal microscope (Radiance 2000; Bio-Rad).

Rice Transformation

The transformation of *Pro_{35S}:Sgr-GFP* in the pCAMLA vector into the mature embryos of *sgr* seeds was performed by the *Agrobacterium tumefaciens*–mediated cocultivation method as described previously (Jeon et al., 2000). The transgenic rice plants were regenerated from the transformed calli on selection medium containing 40 mg/L hygromycin B.

In Vitro Chl Binding Assay

For the in vitro Chl binding assay, 500 pmol of the purified MBP, MBP-ΔSgr, and MBP-ΔWSCP fusions (Δ indicates the removal of N-terminal chloroplast-transit amino acids) was mixed with 500 pmol of spinach (*Spinacia oleracea*) Chls in Chl binding buffer (10 mM sodium phosphate, pH 7.2, and 20% ethanol) at 22°C for 1 h. The mixtures were subjected to 10% native PAGE, and Chl fluorescence was examined under long-waved UV light as described previously (Satoh et al., 1998). The purified MBP was used as a negative control, and the MBP-ΔWSCP (cauliflower) fusion protein obtained from H. Satoh (Satoh et al., 1998) was used as a positive control.

In Vitro Assay of Chlorophyllase Activity

Two milliliters of the purified GST-Sgr fusion, the GST-At CLH2 fusion, or GST (20 μg/mL) was mixed with 4 mL of 0.1 M MOPS buffer, pH 7.0, and 2 mL of acetone containing Chls purified from spinach as described previously (Iriyama et al., 1974; Jacob-Wilk et al., 1999; Benedetti and Arruda, 2002). The reaction mixture was incubated at 25°C for different time periods, and the reaction (0.5 mL) was stopped by transferring to 0.5 mL of hexane plus 0.5 mL of acetone, vortexed vigorously, and then centrifuged at maximum speed for 2 min for phase separation. The Chlide content was determined by measuring the increase of absorbance at 667 nm in the phase-separated acetone layer.

Transient Overexpression in *Nicotiana benthamiana* by *Agrobacterium* Infiltration

Agrobacterium infiltration was performed in the leaves of *N. benthamiana* with *Agrobacterium* strain LBA4404 carrying *Pro_{35S}:Sgr* or *Pro_{35S}:sgr* in pCAMBIA 1300 or *Pro_{35S}:GFP* in pCAMLA vector as described (Llave et al., 2000). The recombinant agrobacteria were initially grown in 5 mL of Luria-Bertani liquid medium at 28°C for 2 d and then subcultured to 50 mL of Luria-Bertani liquid medium supplemented with 10 mM MES, pH 5.6, and 40 μM acetosyringone. When the growth achieved 1.0 OD_{600}, the agrobacteria were pelleted by centrifugation, resuspended in 50 mL of the *Agrobacterium* infiltration buffer (10 mM $MgCl_2$, 10 mM MES, pH 5.6, and 150 μM acetosyringone), and then kept at room temperature for 3 h. After incubation, the *Agrobactrium* buffer was infiltrated into the leaves of 3- to 4-week-old *N. benthamiana* plants with a 1-mL syringe. Symptom development was monitored from 2 d after infiltration.

In Vitro Pull-Down Assay

To examine the in vitro interaction between Sgr and LHCPs, 5 μg of the purified MBP-ΔSgr fusion or MBP protein was mixed with the in vitro binding buffer containing 100 μg of total soluble protein of rice and incubated at 22°C for 1 h. The in vitro binding buffer (50 mM Tris-HCl, pH 7.5, 0.15 M NaCl, 1 mM DTT, 0.5% Triton X-100, and 1 mM phenylmethylsulfonyl fluoride) was used for the extraction of total soluble protein from young leaf tissues of rice. Following immobilization of the MBP fusion protein using amylose resin (New England Biolabs), the resins were vigorously washed three to four times with the binding buffers. The bound proteins were resolved by SDS-PAGE for immunoblot analysis using an anti-MBP antibody. The purified MBP was used as a negative control.

In Vivo Pull-Down Assay

For the in vivo binding assay, *Agrobacterium* strain LBA4404 carrying *Pro_{35S}:Sgr-GST* or *Pro_{35S}:GST* in the pMBP-1 vector and *Pro_{35S}:sgr-GFP* or *Pro_{35S}:GFP* in the pCAMLA vector was infiltrated in the leaves of *N. benthamiana*. At 4 d after infiltration, the leaves were ground with liquid nitrogen and sonicated with a Sonic Dismembrator (model 100; Fischer Scientific) after being mixed with the in vivo binding buffer (50 mM Tris-HCl, pH 7.5, 0.15 M NaCl, 0.2% Triton X-100, 1 mM DTT, and Complete protease inhibitor cocktail [Roche]). After centrifugation, the Sgr-GST or GST protein was pulled down using glutathione Sepharose beads. The pulled-down beads were washed at least three times with the binding buffer, and then copurified proteins were eluted with 10 mM glutathione in 50 mM Tris-HCl, pH 8.0. The eluted proteins were resolved by SDS-PAGE for immunoblot analysis. For GFP coimmunoprecipitation assay, the Rabbit TrueBlot set was used according to the manufacturer's manual (eBioscience). One milligram of total soluble protein was precleared by adding 50 μL of anti-rabbit IgG beads, and then 5 μL of anti-GFP antibody (Abcam) was added to the precleared leaf extracts. After 1 h of incubation on ice, 50 μL of anti-rabbit IgG beads was added and incubated for 1 h. The beads were washed three times with the in vivo binding buffer and boiled in SDS sample buffer. Following SDS-PAGE and transfer to a PVDF membrane, the GFP-bound proteins were detected by immunoblot analysis with the Rabbit IgG TrueBlot system (eBioscience).

Accession Numbers

The GenBank accession numbers of rice *Sgr* and its homologs in other plants are as follows: rice *Sgr* (Os09g36200), AY850134; barley *Sgr*, AY850135; maize *Sgr1*, AY850136; maize *Sgr2*, AY850137; sorghum *Sgr*, AY850140; *Zoysia Sgr1*, AY850154; *Arabidopsis SGN1* (At4g22920), AY850161; *Arabidopsis SGN2* (At4g11910), AY699948; soybean *Sgr1*, AY850141; soybean *Sgr2*, AY850142; and tomato *Sgr1*, DQ100158.

Supplemental Data

The following materials are available in the online version of this article.

Supplemental Figure 1. ClustalW Alignments and Phylogenetic Tree of Sgr Proteins in Higher Plants.

Supplemental Figure 2. Subcellular Localization of the Sgr-GFP Fusion in *Arabidopsis* Protoplasts.

Supplemental Figure 3. Evaluation of Rice SAG Expression in Detached Leaves during Dark-Induced Senescence.

Supplemental Figure 4. In Vitro Chl Binding Assay.

Supplemental Figure 5. In Vitro Assay for Chlorophyllase Activity.

Supplemental Figure 6. Negative Controls for the Transient Overexpression Assay in *N. benthamiana*.

Supplemental Table 1. PCR Primers Used in This Study.

ACKNOWLEDGMENTS

We thank N.-S. Jwa for donating the pCAMLA vector, D. Choi for the pMBP-1 vector, H. Satoh for the recombinant MBP-ΔWSCP plasmid, S. Hörtensteiner for the *pao1* seeds, the Rice Genome Research Program for RFLP markers, and the ABRC for *acd1-20* seeds. This work was supported by Grant CG3131 from the Crop Functional Genomics Center of the 21st Century Frontier Research Program, funded by the Ministry of Science and Technology and Rural Development Administration of the Republic of Korea.

Received June 13, 2006; revised March 28, 2007; accepted May 2, 2007; published May 18, 2007.

REFERENCES

Akhtar, M.S., Goldschmidt, E., John, I., Rodoni, S., Matile, P., and Grierson, D. (1999). Altered patterns of senescence and ripening in *gf*, a stay-green mutant of tomato (*Lycopersicon esculentum* Mill.). J. Exp. Bot. **50:** 1115–1122.

Armstead, I., et al. (2006). From crop to model to crop: Identifying the genetic basis of the staygreen mutation in the *Lolium/Festuca* forage and amenity grasses. New Phytol. **172:** 592–597.

Armstead, I., et al. (2007). Cross-species identification of Mendel's *I* locus. Science **315:** 73.

Benedetti, C.E., and Arruda, P. (2002). Altering the expression of the chlorophyllase gene *ATHCOR1* in transgenic Arabidopsis caused changes in the chlorophyll-to-chlorophyllide ratio. Plant Physiol. **128:** 1255–1263.

Benedetti, C.E., Costa, C.L., Turcinelli, S.R., and Arruda, P. (1998). Differential expression of a novel gene in response to coronatine, methyl jasmonate, and wounding in the *Coi1* mutant of Arabidopsis. Plant Physiol. **116:** 1037–1042.

Brandis, A., Vainstein, A., and Goldschmidt, E.E. (1996). Distribution of chlorophyllase among components of chloroplast membranes in *Citrus sinensis* organs. Plant Physiol. Biochem. **40:** 111–118.

Buchanan-Wollaston, V. (1997). The molecular biology of leaf senescence. J. Exp. Bot. **33:** 821–834.

Cha, K.-W., Lee, Y.-J., Koh, H.-J., Lee, B.-M., Nam, Y.-W., and Paek, N.-C. (2002). Isolation, characterization, and mapping of the stay green mutant in rice. Theor. Appl. Genet. **104:** 526–532.

Cheung, A.Y., McNellis, T., and Piekos, B. (1993). Maintenance of chloroplast components during chromoplast differentiation in the tomato mutant *Green Flesh*. Plant Physiol. **101:** 1223–1229.

Efrati, A., Eyal, Y., and Paran, I. (2005). Molecular mapping of the *chlorophyll retainer* (*cl*) mutation in pepper (*Capsicum* spp.) and screening for candidate genes using tomato ESTs homologous to structural genes of the chlorophyll catabolism pathway. Genome **48:** 347–351.

Emanuelsson, O., Nielsen, H., Brunak, S., and von Heijne, G. (2000). Predicting subcellular localization of proteins based on their N-terminal amino acid sequence. J. Mol. Biol. **300:** 1005–1016.

Emanuelsson, O., Nielsen, H., and von Heijne, G. (1999). ChloroP, a neural network-based method for predicting chloroplast transit peptides and their cleavage sites. Protein Sci. **8:** 978–984.

Fang, Z., Bouwkamp, J.C., and Solomos, T. (1998). Chlorophyllase activities and chlorophyll degradation during leaf senescence in non-yellowing mutant and wild type of *Phaseolus vulgaris* L. J. Exp. Bot. **49:** 503–510.

Garcia-Lorenzo, M., Żelisco, A., Jackowski, G., and Funk, C. (2005). Degradation of the main photosystem II light-harvesting complex. Photochem. Photobiol. Sci. **4:** 1065–1071.

Gindullis, F., and Meier, I. (1999). Matrix attachment region binding protein MFP1 is localized in discrete domains at the nuclear envelope. Plant Cell **11:** 1117–1128.

Gray, J., Close, P.S., Briggs, S.P., and Johal, G.S. (1997). A novel suppressor of cell death in plants encoded by the *Lls1* gene of maize. Cell **89:** 25–31.

Gray, J., Janick-Bruckner, D., Bruckner, B., Close, P.S., and Johal, G.S. (2002). Light-dependent death of maize lls1 cells is mediated by mature chloroplasts. Plant Physiol. **130:** 1894–1907.

Greenberg, J.T., and Ausubel, F.M. (1993). Arabidopsis mutants compromised for the control of cellular damage during pathogenesis and aging. Plant J. **4:** 327–341.

Guiamét, J.J., Pichersky, E., and Noodén, L.D. (1999). Mass exodus from senescing soybean chloroplasts. Plant Cell Physiol. **40:** 986–992.

Guiamét, J.J., Schwartz, E., Pichersky, E., and Noodén, L.D. (1991). Characterization of cytoplasmic and nuclear mutations affecting chlorophyll and chlorophyll-binding proteins during senescence in soybean. Plant Physiol. **96:** 227–231.

Guiamét, J.J., Tyystjärvi, E., Tyystjärvi, T., John, I., Kairavuo, M., Pichersky, E., and Noodén, L.D. (2002). Photoinhibition and loss of photosystem II reaction center proteins during senescence of soybean leaves. Enhancement of photoinhibition by the 'stay-green' mutation *cytG*. Physiol. Plant. **115:** 468–478.

Hilditch, P. (1986). Immunological qualification of the chlorophyll *a*/*b* binding protein in senescing leaves of *Festuca pratensis* Huds. Plant Sci. **45:** 95–99.

Hilditch, P., Thomas, H., Thomas, B.J., and Rogers, L.J. (1989). Leaf senescence in a non-yellowing mutant of *Festuca pratensis*: Proteins of photosystem II. Planta **177:** 265–272.

Hörtensteiner, S. (2006). Chlorophyll degradation during senescence. Annu. Rev. Plant Biol. **57:** 55–77.

Hörtensteiner, S., and Feller, U. (2002). Nitrogen metabolism and remobilization during senescence. J. Exp. Bot. **53:** 927–937.

Hörtensteiner, S., and Matile, P. (2004). How leaves turn yellow: Catabolism of chlorophyll. In Plant Cell Death Processes, L.D. Noodén, ed (San Diego, CA: Academic Press), pp. 189–202.

Inada, N., Sakai, A., Kuroiwa, H., and Kuroiwa, T. (1998). Three-dimensional analysis of the senescence program in rice (*Oryza sativa* L.) coleoptile. Investigation by fluorescence microscopy and electron microscopy. Planta **206:** 585–597.

Iriyama, K., Ogura, N., and Takamiya, A. (1974). A simple method for extraction and partial purification of chlorophyll from plant material, using dioxane. J. Biochem. (Tokyo) **76:** 901–904.

Jacob-Wilk, D., Holland, D., Goldschmidt, E.E., Riov, J., and Eyal, Y. (1999). Chlorophyll breakdown by chlorophyllase: Isolation and functional expression of the *Chlase1* gene from ethylene-treated *Citrus* fruit and its regulation during development. Plant J. **20:** 653–661.

Jeon, J.-S., et al. (2000). T-DNA insertional mutagenesis for functional genomics in rice. Plant J. **22:** 561–570.

Lee, J.-H., Kim, S.-H., Jung, Y.-H., Kim, J.-A., Lee, M.-O., Choi, P.-G., Choi, W., Kim, K.-N., and Jwa, N.-S. (2005). Molecular cloning and functional analysis of rice (*Oryza sativa* L.) *OsNDR1* on defense signaling pathway. Plant Pathol. J. **21:** 149–157.

Lee, R.-H., Wang, C.-H., Huang, L.-T., and Chen, S.-C.G. (2001). Leaf senescence in rice plants: Cloning and characterization of senescence up-regulated genes. J. Exp. Bot. **52:** 1117–1121.

Lim, **P.O.**, **and Nam**, **H.G.** (2005). The molecular and genetic control of leaf senescence and longevity in *Arabidopsis*. Curr. Top. Dev. Biol. **67:** 49–83.

Llave, **C.**, **Kasschau**, **K.D.**, **and Carrington**, **J.C.** (2000). Virus-encoded suppressor of posttranscriptional gene silencing targets a maintenance step in the silencing pathway. Proc. Natl. Acad. Sci. USA **97:** 13401–13406.

Mach, **J.M.**, **Castillo**, **A.R.**, **Hoogstraten**, **R.**, **and Greenberg**, **J.T.** (2001). The *Arabidopsis*-accelerated cell death gene *ACD2* encodes red chlorophyll catabolite reductase and suppresses the spread of disease symptoms. Proc. Natl. Acad. Sci. USA **98:** 771–776.

Matile, **P.**, **Ginsburg**, **S.**, **Schellenberg**, **M.**, **and Thomas**, **H.** (1988). Catabolites of chlorophyll in senescing barley gerontoplasts. Plant Physiol. Biochem. **34:** 55–59.

Matile, **P.**, **Hörtensteiner**, **S.**, **and Thomas**, **H.** (1999). Chlorophyll degradation. Annu. Rev. Plant Physiol. Plant Mol. Biol. **50:** 67–95.

Matile, **P.**, **Schellenberg**, **M.**, **and Vicentini**, **F.** (1997). Localization of chlorophyllase in the chloroplast envelope. Planta **201:** 96–99.

Nam, **H.G.** (1997). The molecular genetic analysis of leaf senescence. Curr. Opin. Biotechnol. **8:** 200–207.

Noodén, **L.D.**, **Guiamét**, **J.J.**, **and John**, **I.** (1997). Senescence mechanisms. Physiol. Plant. **101:** 746–753.

Oh, **M.-H.**, **Kim**, **Y.-J.**, **and Lee**, **C.-H.** (2000). Leaf senescence in a stay-green mutant of *Arabidopsis thaliana*: Disassembly process of photosystem I and II during dark-incubation. J. Biochem. Mol. Biol. **33:** 256–262.

Oh, **M.-H.**, **Moon**, **Y.-H.**, **and Lee**, **C.-H.** (2003). Increased stability of LHCII by aggregate formation during dark-induced leaf senescence in the *Arabidopsis* mutant, *ore10*. Plant Cell Physiol. **44:** 1368–1377.

Oh, **M.-H.**, **Safarova**, **R.B.**, **Zulfugarov**, **I.S.**, **Park**, **T.-S.**, **Choi**, **K.-J.**, **and Lee**, **C.-H.** (2006). ORE10, a protein that regulates stay-greenness in *Arabidopsis*. Korean J. Crop Sci. **51** (suppl. 2): 143.

Okazawa, **A.**, **Tang**, **L.**, **Itoh**, **Y.**, **Fukusaki**, **E.**, **and Kobayashi**, **A.** (2006). Characterization and subcellular localization of chlorophyllase from *Ginkgo biloba*. Z. Naturforsch. **61c:** 111–117.

Pružinská, **A.**, **Tanner**, **G.**, **Anders**, **I.**, **Roca**, **M.**, **and Hörtensteiner**, **S.** (2003). Chlorophyll breakdown: Pheophorbide *a* oxygenase is a Rieske-type iron–sulfur protein, encoded by the *accelerated cell death 1* gene. Proc. Natl. Acad. Sci. USA **100:** 15259–15264.

Pružinská, **A.**, **Tanner**, **G.**, **Aubry**, **S.**, **Anders**, **I.**, **Moser**, **S.**, **Müller**, **T.**, **Ongania**, **K.-H.**, **Kräutler**, **B.**, **Youn**, **J.-Y.**, **Liljegren**, **S.J.**, **and Hörtensteiner**, **S.** (2005). Chlorophyll breakdown in senescent Arabidopsis leaves. Characterization of chlorophyll catabolites and chlorophyll catabolic enzymes involved in the degreening reaction. Plant Physiol. **139:** 52–63.

Reinbothe, **C.**, **Satoh**, **H.**, **Alcaraz**, **J.P.**, **and Reinbothe**, **S.** (2004). A novel role of water-soluble chlorophyll proteins in the transitory storage of chlorophyllide. Plant Physiol. **134:** 1355–1365.

Reyes-Arribas, **T.**, **Barrett**, **J.E.**, **Huber**, **D.J.**, **Nell**, **T.A.**, **and Clark**, **D.G.** (2001). Leaf senescence in a non-yellowing cultivar of chrysanthemum (*Dendranthema grandiflora*). Physiol. Plant. **111:** 540–544.

Roca, **M.**, **James**, **C.**, **Pružinská**, **A.**, **Hörtensteiner**, **S.**, **Thomas**, **H.**, **and Ougham**, **H.** (2004). Analysis of the chlorophyll catabolism pathway in leaves of an introgression senescence mutant of *Lolium temulentum*. Phytochemistry **65:** 1231–1238.

Roca, **M.**, **and Mínguez-Mosquera**, **M.I.** (2006). Chlorophyll catabolism pathway in fruits of *Capsicum annuum* (L.): stay-green versus red fruits. J. Agric. Food Chem. **54:** 4035–4040.

Satoh, **H.**, **Nakayama**, **K.**, **and Okada**, **M.** (1998). Molecular cloning and functional expression of a water-soluble chlorophyll protein, a putative carrier of chlorophyll molecules in cauliflower. J. Biol. Chem. **273:** 30568–30575.

Takamiya, **K.**, **Tsuchiya**, **T.**, **and Ohta**, **H.** (2000). Degradation pathway(s) of chlorophyll: What has gene cloning revealed? Trends Plant Sci. **5:** 426–431.

Tanaka, **R.**, **Hirashima**, **M.**, **Satoh**, **S.**, **and Tanaka**, **A.** (2003). The *Arabidopsis-accelerated cell death* gene *ACD1* is involved in oxygenation of pheophorbide *a*: Inhibition of the pheophorbide *a* oxygenase activity does not lead to the ''stay-green'' phenotype in *Arabidopsis*. Plant Cell Physiol. **44:** 1266–1274.

Tang, **L.**, **Okazawa**, **A.**, **Itoh**, **Y.**, **Fukusaki**, **E.**, **and Kobayashi**, **A.** (2004). Expression of chlorophyllase is not induced during autumnal yellowing in *Ginkgo biloba*. Z. Naturforsch. **59c:** 415–420.

Thomas, **H.** (1977). Ultrastructure, polypeptide composition and photochemical activity of chloroplasts during foliar senescence of a non-yellowing mutant genotype of *Festuca pratensis* Huds. Planta **137:** 53–60.

Thomas, **H.** (1982). Leaf senescence in a non-yellowing mutant of *Festuca pratensis*. I. Chloroplast membrane polypeptides. Planta **154:** 212–218.

Thomas, **H.**, **Bortlik**, **K.**, **Rentsch**, **D.**, **Schellenberg**, **M.**, **and Matile**, **P.** (1989). Catabolism of chlorophyll *in vivo*: Significance of polar chlorophyll catabolites in a non-yellowing senescence mutant of *Festuca pratensis* Huds. New Phytol. **111:** 3–8.

Thomas, **H.**, **and Howarth**, **C.J.** (2000). Five ways to stay green. J. Exp. Bot. **51:** 329–337.

Thomas, **H.**, **Ougham**, **H.**, **Canter**, **P.**, **and Donnison**, **I.** (2002). What stay-green mutants tell us about nitrogen remobilization in leaf senescence. J. Exp. Bot. **53:** 801–808.

Thomas, **H.**, **and Smart**, **C.M.** (1993). Crops that stay green. Ann. Appl. Biol. **123:** 193–219.

Thomas, **H.**, **and Stoddart**, **J.** (1975). Separation of chlorophyll degradation from other senescence processes in leaves of a mutant genotype of meadow fescue (*Festuca pratensis* L.). Plant Physiol. **56:** 438–441.

Tsuchiya, **T.**, **Ohta**, **H.**, **Okawa**, **K.**, **Iwamatsu**, **A.**, **Shimada**, **H.**, **Masuda**, **T.**, **and Takamiya**, **K.** (1999). Cloning of chlorophyllase, the key enzyme in chlorophyll degradation: Finding of a lipase motif and the induction by methyl jasmonate. Proc. Natl. Acad. Sci. USA **96:** 15362–15367.

Vicentini, **F.**, **Hörtensteiner**, **S.**, **Schellenberg**, **M.**, **Thomas**, **H.**, **and Matile**, **P.** (1995). Chlorophyll breakdown in senescing leaves: Identification of the biochemical lesion in a stay-green genotype of *Festuca pratensis* Huds. New Phytol. **129:** 247–252.

White, **M.J.**, **and Green**, **B.R.** (1987). Polypeptides belonging to each of the three major chlorophyll $a + b$ protein complexes are present in a chlorophyll-*b*-less barley mutant. Eur. J. Biochem. **165:** 531–535.

Yi, **S.Y.**, **Kim**, **J.-H.**, **Joung**, **Y.-H.**, **Lee**, **S.**, **Kim**, **W.-T.**, **Yu**, **S.H.**, **and Choi**, **D.** (2004). The pepper transformation factor CaPF1 confers pathogen and freezing tolerance in Arabidopsis. Plant Physiol. **136:** 2862–2874.

Żelisko, **A.**, **Garcia-Lorenzo**, **M.**, **Jackowski**, **G.**, **Jansson**, **S.**, **and Funk**, **C.** (2005). AtFtsH6 is involved in the degradation of the light-harvesting complex II during high-light acclimation and senescence. Proc. Natl. Acad. Sci. USA **102:** 13699–13704.

Zimmermann, **P.**, **Hirsch-Hoffmann**, **M.**, **Hennig**, **L.**, **and Gruissem**, **W.** (2004). GENEVESTIGATOR. Arabidopsis microarray database and analysis toolbox. Plant Physiol. **136:** 2621–2632.